NAVAL POSTGRADUATE SCHOOL

MONTEREY, CALIFORNIA

THESIS

CLASSIFICATION OF DIGITAL MODULATION TYPES IN MULTIPATH ENVIRONMENTS

by

Andrew Fraser Young

June 2008

Thesis Advisor:	Monique P. Fargues
Second Reader:	Roberto Cristi

THIS PAGE INTENTIONALLY LEFT BLANK

REPORT DOCUMENTATION PAGE			Form Approved OMB No. 0704-0188
Public reporting burden for this collection of information is estimated to average 1 hour per response, including the time for reviewing instruction, searching existing data sources, gathering and maintaining the data needed, and completing and reviewing the collection of information. Send comments regarding this burden estimate or any other aspect of this collection of information, including suggestions for reducing this burden, to Washington headquarters Services, Directorate for Information Operations and Reports, 1215 Jefferson Davis Highway, Suite 1204, Arlington, VA 22202-4302, and to the Office of Management and Budget, Paperwork Reduction Project (0704-0188) Washington DC 20503.			
1. AGENCY USE ONLY *(Leave blank)*	**2. REPORT DATE** June 2008	**3. REPORT TYPE AND DATES COVERED** Master's Thesis	
4. TITLE AND SUBTITLE Classification of Digital Modulation Types in Multipath Environments		**5. FUNDING NUMBERS**	
6. AUTHOR(S) Young, Andrew F.			
7. PERFORMING ORGANIZATION NAME(S) AND ADDRESS(ES) Naval Postgraduate School Monterey, CA 93943-5000		**8. PERFORMING ORGANIZATION REPORT NUMBER**	
9. SPONSORING /MONITORING AGENCY NAME(S) AND ADDRESS(ES) N/A		**10. SPONSORING/MONITORING AGENCY REPORT NUMBER**	
11. SUPPLEMENTARY NOTES The views expressed in this thesis are those of the author and do not reflect the official policy or position of the Department of Defense or the U.S. Government.			
12a. DISTRIBUTION / AVAILABILITY STATEMENT Approved for public release; distribution unlimited		**12b. DISTRIBUTION CODE**	

13. ABSTRACT (maximum 200 words)

As the digital communications industry continues to grow and evolve, the applications of this discipline continue to grow as well. This growth, in turn, has spawned an increasing need to seek automated methods of classifying digital modulation types. This research is a revision of previous work, using the latest mathematical software including MATLAB version 7 and Simulink ®. The program considers the classification of nine different modulation types. Specifically, the classification scheme can differentiate between 2, 4, and 8 PSK, 256-QAM from other types of M-QAM signals, and also M-FSK signals from PSK and QAM signals in various types of propagation channels, including multipath fading and a variety of signal-to-noise levels. This method successfully identifies these modulation types without the benefit of a priori information. Higher-order statistical parameters are selected as class features and are tested in a classifier for their ability to identify the above modulation types. This study considers the effects due to realistic multipath propagation channels and additive white Gaussian noise. Using these features, and considering all fading conditions, it was determined that the classifier was correct for a randomly sent signal under randomly high or low SNR levels (low: 0dB to 8dB; high: 50dB to 100dB) over 83.9% of the time.

14. SUBJECT TERMS Digital modulation, Propagation channels, Moments, Cumulants, Classification, Simulink , PSK, FSK, QAM			**15. NUMBER OF PAGES** 83
			16. PRICE CODE
17. SECURITY CLASSIFICATION OF REPORT Unclassified	**18. SECURITY CLASSIFICATION OF THIS PAGE** Unclassified	**19. SECURITY CLASSIFICATION OF ABSTRACT** Unclassified	**20. LIMITATION OF ABSTRACT** UU

NSN 7540-01-280-5500 Standard Form 298 (Rev. 2-89)
Prescribed by ANSI Std. 239-18

THIS PAGE INTENTIONALLY LEFT BLANK

Approved for public release; distribution is unlimited

CLASSIFICATION OF DIGITAL MODULATION TYPES IN MULTIPATH ENVIRONMENTS

Andrew F. Young
Lieutenant, United States Navy
B.S., Kansas State University, 1999

Submitted in partial fulfillment of the
requirements for the degree of

MASTER OF SCIENCE IN ELECTRICAL ENGINEERING

from the

NAVAL POSTGRADUATE SCHOOL
June 2008

Author: Andrew F. Young

Approved by: Monique P. Fargues
Thesis Advisor

Roberto Cristi
Second Reader

Jeffery B. Knorr
Chairman, Department of Electrical and Computer Engineering

THIS PAGE INTENTIONALLY LEFT BLANK

ABSTRACT

As the digital communications industry continues to grow and evolve, the applications of this discipline continue to grow as well. This growth, in turn, has spawned an increasing need to seek automated methods of classifying digital modulation types. This research is a revision of previous work, using the latest mathematical software including MATLAB version 7 and Simulink ®. The program considers the classification of nine different modulation types. Specifically, the classification scheme can differentiate between 2,- 4, and 8 PSK, 256-QAM from other types of M-QAM signals, and also M-FSK signals from PSK and QAM signals in various types of propagation channels, including multipath fading and a variety of signal-to-noise levels. This method successfully identifies these modulation types without the benefit of a priori information. Higher-order statistical parameters are selected as class features and are tested in a classifier for their ability to identify the above modulation types. This study considers the effects due to realistic multipath propagation channels and additive white Gaussian noise. Using these features, and considering all fading conditions, it was determined that the classifier was correct for a randomly sent signal under randomly high or low SNR levels (low: 0dB to 8dB; high: 50dB to 100dB) over 83.9% of the time.

THIS PAGE INTENTIONALLY LEFT BLANK

TABLE OF CONTENTS

LIST OF FIGURES

THIS PAGE INTENTIONALLY LEFT BLANK

LIST OF TABLES

THIS PAGE INTENTIONALLY LEFT BLANK

EXECUTIVE SUMMARY

The classification of digital modulation techniques is a desired element of multiple organizations, companies, and governmental organizations, in order to develop a universal demodulation device. This process of identifying the digital modulation type of a given signal with various conditions of noise, distortion, and attenuation can bring the user one step closer to fully identifying and thus manipulating, identifying, and processing the signal. The signals intelligence community would especially find this useful to facilitate identifying signals and using that information to facilitate extrapolating actionable intelligence for military targets of interest.

This research is based on the work of [1] which proposed using statistical features in concert with a neural network classification tree to identify unknown signals through various propagation channels. Using the latest available version of MATLAB (R2007a) and Simulink ®, this revision of a digital modulation classification program will take a user-chosen modulation type (M-PSK, M-FSK, or M-QAM), propagate it through noise, and finally tell the user what the modulation type was. In this effort, the classification program consists of threshold values based on user selected specific higher order statistical features. Using the higher order moments and cumulants features selected, it was discovered that the 16- and 64-QAM signals are more difficult to distinguish from one another. Also the M-FSK signals are unable to be distinguished from one another due to the similarities in their respective higher order statistical features. This research investigates the robustness of the proposed scheme to distortion due to noisy channels and of SNR levels of lower values ranging from 0dB to 8dB and higher values ranging from 50dB to 100dB.

THIS PAGE INTENTIONALLY LEFT BLANK

ACKNOWLEDGMENTS

First, I would like to thank my wife, Kelly, and our three boys, Logan, Aaron, and Jacob. Without their support, prayers, and belief in me, I might have been graduating much, much later than originally anticipated. Thank you especially to my mom and dad and my in-laws, Larry and Patti, for helping with everything else that needs to be done in life besides writing a thesis. I would also like to thank my friends and prayer warriors at the local church, your prayers were truly answered in this thesis. Shoreline sermons often presented inspiration and hope when I needed it the most. Keith and Shannon Krueger were always there for us, despite their busy schedules. A special thank you needs to go out to Capt Jameson McGee, USMC, who helped me out with a very important skill: debugging. Finally, I dedicate this thesis to my Lord and Savior, Jesus Christ. If it were not for him, I would not be where I am today and my future could only be a series of uncertain guesses at best.

THIS PAGE INTENTIONALLY LEFT BLANK

I. INTRODUCTION

A. THESIS OBJECTIVES

For many years, corporations and governments have desired to develop a universal digital modulation identification feature in their analog and digital communications systems. As the telecommunications industry continues to grow at an exponential rate, the benefits in terms of both cost and utility of such a device would improve the functionality of networks and communications systems globally. This thesis investigates the robustness and capabilities of a digital modulation classifier, which uses the statistical features of higher order moments and cumulants. The modulation types considered include M-ary phase shift keying (M-PSK), M-ary frequency shift keying (M-FSK), and M-ary Quadrature Amplitude Modulation (M-QAM). Much work has already been done since the 1960s and continues in increasing number and scope of research to this day. However, much of the previous work in this particular area of communications research has used either simplified propagation channels, usually assuming only additive white Gaussian noise, or includes only a limited number of modulation types. This thesis study considers the classification of nine different modulation types. Specifically, the classification scheme will be able differentiate between M-PSK, M-QAM and also M-FSK signals in various types of propagation channels, including multipath fading and SNR levels ranging from 0dB to noise-free channel models.

B. BACKGROUND

Governments, corporations, military organizations, non-governmental agencies, and interested individuals all share an interest in classifying digital modulation types in noise. Such classification tools play an important role in electronic surveillance systems, military communications, emitter interception, signal verification, and interference identification. From an intelligence perspective, modulation classification is also a useful first step in further classifying, analyzing, decoding, and ultimately acquiring the communications message. Attempts have been made since the early 1960s to classify

digital modulation types in various types of propagation channels and noise, and using various features of the signals of interest. The following list of papers is based on much of this research, and each year there are dozens more than what is listed here.

In 1984, Liedtke [2] described a computer simulation of an automatic classification procedure for digitally modulated communication signals with known parameters. This article focused on binary ASK, binary FSK, and the three types of PSK (i.e., two, four, and eight) used in this thesis. However, the classification procedure was conducted on a Burroughs B5500 computer, which of course was not as fast as the vast majority of today's computers.

In 1997, Le Martret and Boiteaut [3] dealt with the modulation classification of 4-PSK and 16-QAM using a combination of fourth and second order moments. However, considering modern communications utilize a far greater number of modulation types, the work in this thesis considers multiple variations of QAM and PSK as well as FSK modulation types.

In 1998, Marchand [4] attempted to automate the detection and recognition of QAM and PSK digital modulations by using cyclical statistics of higher order.

In 1999, Taira and Murakami [5] proposed an approach to classify analog frequency and amplitude modulation types using first and second order moments. However, their proposed automatic classification program was primarily used to first distinguish between analog and digital signals. Their classification program then would only actually attempt to classify the analog case, while the digital case was not classified. Given the sheer volume of digital communications, this work seems dated at best.

In 2000, Wei and Mendel [6] applied the maximum-likelihood method to classify QAM and other amplitude modulated signals under AWGN conditions. Their assumptions and work led to the classification of QAM signals with no errors. However, their computer simulations used mathematical models which all assume an infinite amount of data symbols and was not yet ready for realistic, multipath faded finite signals in significantly more challenging environments.

In 2001, Hatzichristos [1] proposed a neural network based classification scheme to be used in the classification of modulation types. However, the higher order moments and cumulants of the frequency shift keying (FSK) results did not match the work of others, including [4] and some of the tables of data in [1] occasionally were not accurate. This in turn motivated the need for a second look at the work and the resulting model presented in this research.

In 2002, Kalinin and Kavalov [7] used a neural network for automatic recognition of two types of digital passband modulations. A feed-forward network with six hidden neurons was trained to recognize BPSK and minimum shift keying signals. The performance of the classifier was tested in the presence of additive white Gaussian noise between SNR levels of 10dB to 12dB, showing a 95% to 99% correct recognition rate. However the simulations for SNR levels outside of this range were not reported. Additionally, FSK and QAM were ignored, and AWGN is not an appropriate realistic channel model in urban or rural environments.

In 2004, Dobre, Wei, and Bar-Ness [8] developed an algorithm based on higher-order cyclic cumulants for the automatic recognition of QAM signals. Their method is robust to the presence of carrier phase and frequency offsets. Their theoretical arguments were verified with simulations performed for 4-QAM and 16-QAM signals. However, again the world of digital modulation is much richer than just QAM signals.

In 2006, Baarrij, Nasir; and Masood [9] developed an automatic modulation recognition model using linear approximation features for real-time classification of digitally modulated signals without any prior knowledge of signal parameters. Basic FSK, PSK, ASK, QAM, and Gaussian minimum shift keying (GMSK) modulation types were detected and the order identified in a hierarchical fashion. Their simulations showed 99.9% recognition rates for SNR levels as low as 5 dB. However, no multipath fading and only AWGN distortion was considered in their work. These developments and many others have led in this study to a potentially robust MATLAB-based implementation using Simulink ® (R2007a) to classify modulation types.

C. SOFTWARE UTILIZED

MATLAB version 7.4.0 (R2007a) was used in concert with Simulink ® version 6.6 (R2007a) to generate the data and conduct the simulations while Excel 2003 was utilized to store all simulation results. Realistic conditions of various multipath environments were simulated using Rayleigh and Ricean channel block sets in Simulink.

D. THESIS ORGANIZATION

Some of the organization and research efforts of this thesis will parallel that found in [1], which is the basis from which this research begins. However, the use of neural networks and constant modulus algorithms used in [1] were not utilized in this work. Chapter I, section C will provide a review of some of the many research efforts that have been made in the digital modulation classification area. Chapter II provides a brief introduction to digital communication systems. Within this introduction, we take a look at nine different modulation types commonly used. Chapter III provides an introduction to additive white Gaussian noise as well as two types of multipath fading in the transmission channel: Ricean and Rayleigh fading. Chapter IV introduces the concept of higher-order statistics with emphasis on higher-order statistical moments and cumulants. These statistical parameters are selected as identification features in the classification scheme. We investigate the robustness of these features with respect to propagation problems. Chapter V discusses the revised classifier software implementation and the corresponding Simulink models are described and evaluated with simulations. Chapter VI provides a summary of the results corresponding to the success rates of the classifier on PSK, FSK, and QAM signals. Chapter VII provides an overall conclusion of the results as well as future research that may be conducted in this area.

II. DIGITAL COMMUNICATIONS SYSTEMS

This chapter provides an introduction to digital communication systems and the digital modulation techniques studies in this work.

A. INTRODUCTION TO DIGITAL COMMUNICATION SYSTEMS

Figure 1 is a block diagram of a typical digital communication system showing how a communications signal is transmitted from an information source, through a transmitter, through a channel, into a receiver, and to a final destination. The transmitter can be modeled using the blocks in the dashed lines around the boxes representing the formatting of the message, encoding the signal, encryption, encoding the signal to prepare for channel travel, multiplexing, modulating the signal and transmitting it. The grayed out boxes represent some of the common processes, but they are not essential to a communications system. It is essential, however, to format the analog or digital information source and to modulate and transmit the signal if one is to have a working digital communication system. For wireless systems, an antenna is the final ingredient to actually transmit the signal through space.

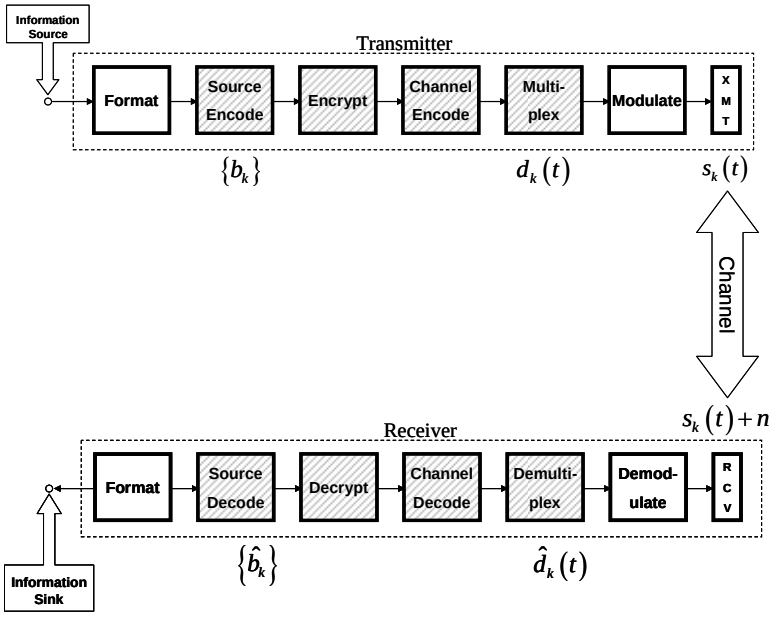

Figure 1. Digital Communication System Model After [10]

When a signal travels through a propagation channel, there are always noises, distortions, reflections, delays, attenuations and other phenomenon which interfere with the signal of interest. One primary source of interference is thermal noise, caused by thermal agitation of electrons, which is present in all electronic devices and is a function of temperature [11]. Thermal noise is usually modeled using additive white Gaussian noise, which is used extensively throughout this thesis. Other types of noise include intermodulation noise, cross-talk, and impulse noise.

Another phenomenon that can occur in the channel, through which a signal is traveling toward its receiver, is fading. Fading occurs when the amplitude and phase of a signal changes rapidly over short periods of time or travel distances. Fading is caused when a signal and a delayed version of itself arrive at the destination at different times. Multipath phenomena result in a received signal that significantly differs in amplitude and phase from that sent. Fading can be caused by buildings, mountains, weather, and other phenomenon that the signal cannot travel through but must bounce off. Fading can also be caused by the transmitter being in relative motion with the receiver, and the resulting Doppler shifts. The two types of fading discussed in this thesis are Rayleigh fading and Ricean fading. The receiver role is simply to undo what the transmitter has done to the signal. At the other end of a successful communication system, the digital output becomes formatted for the other end user to understand what was originally sent.

B. DIGITAL MODULATION TECHNIQUES

1. Introduction

The basic concept behind digital modulation is to identify efficient schemes taking *M* different symbols in a given digital alphabet and transforming them into waveforms that can successfully transmit the data over the transmission channel. In modern digital communications systems, the modem (i.e., *mo*dulate-*dem*odulate) has the responsibility of converting the digital data to analog signals for transmission and from analog signals to digital data for the received signal. Modulation involves changing the amplitude, frequency and/or the phase of the carrier wave traveling over the channel.

There are therefore three basic types of modulation schemes: frequency shift keying (FSK), amplitude shift keying (ASK), and phase-shift keying (PSK). The Quadrature Amplitude Modulated (QAM) signal is an expansion of the amplitude shift keying modulation types. The QAM signal transmits signals by modulating the amplitude of two sinusoidal carrier waves which are orthogonal to each other (which is what "quadrature" means: 90 degrees out of phase). The resulting signal will then exist in a bandwidth centered on the carrier frequency [11].

Some of the most widely used digital modulation techniques are summarized in Table 1. This study will concentrate on M-FSK, 2-PSK, 4-PSK, 8-PSK, and 16-QAM, 64-QAM and 256-QAM modulation schemes. Each of these modulation types is described in more detail in the following subsections.

Linear Modulation Techniques	**Constant Envelope Modulation Techniques**	**Combined Linear and Constant Envelope Modulation Techniques**	**Spread Spectrum Modulation Techniques**
2-PSK: Binary Phase Shift Keying	2-FSK: Binary Frequency Shift Keying	M-PSK: M-ary Phase Shift Keying	DS-SS: Direct Sequence Spread Spectrum
DPSK: Differential Phase Shift Keying	MSK: Minimum Shift Keying	QAM: M-ary Quadrature Amplitude Modulation	FH-SS: Frequency Hopped Spread Spectrum
4-PSK: Quadrature Phase Shift Keying	GMSK: Gaussian Minimum Shift Keying	M-FSK: M-ary Frequency Shift Keying	

Table 1. Popular Digital Modulation Schemes From [1]

2. M-ary Frequency Shift Keying Modulation Scheme

M-ary Frequency Shift Keying (M-FSK) is one of many different kinds of modulation types. FSK modulation is used in many types of digital communications including military communications, like the AN/MRC-145, and historical computer network modems such as the Bell 103, which allowed AT&T to transmit digital computer data over regular telephone wires (c. 1962) [12].

The simplest form of FSK is known as the binary frequency-shift keying (2-FSK), where the symbols 0 and 1 are distinguished from each other using the following sinusoidal carrier formulas

$$\begin{aligned} s_1(t) &= A\cos\left(2\pi f_1 t + \phi\right) \quad \text{binary 1} \\ s_2(t) &= A\cos\left(2\pi f_2 t + \phi\right) \quad \text{binary 0,} \end{aligned} \tag{2.1}$$

where f_1 and f_2 are usually offset from the carrier frequency, f_c, by equal but opposite amounts. For example, in the Bell System 108 series modems, a full-duplex (i.e., signals are sent in both "receive" and "transmit" directions simultaneously) transmission has a carrier frequency of $f_c = 1170\,\text{Hz}$ and the binary 1 is sent at $f_1 = 1070\,\text{Hz}$ while $f_2 = 1270\ \text{Hz}$ [11]. Binary FSK is typically used up to 1200 bps on voice-grade lines. It is also used for high-frequency (3 to 30 MHz) radio transmissions. Additionally, Local Area Networks (LANs) that typically utilize coaxial cable use this BFSK modulation type. Equation 2.1 indicates a *coherent* modulation because the two signals have the same initial phase at the start time of transmission. A *non-coherent* or *discontinuous* modulation occurs when initial phases are different, making the waveform discontinuous at the bit transitions. Non-coherent modulation can be generated by switching the modulator output line between two different oscillators [13]. The advantage of non-coherent over coherent systems is reduced complexity, but the tradeoff is an increased probability of error [10].

A more bandwidth efficient signal (with increased probability of error) is the M-FSK signal where more than two frequencies are used. The number of bits in the binary data stream of ones and zeroes is determined by $n = \log_2(M)$. In this thesis, we study the impact of the classification scheme on *M* different signal elements where *M* = 2, 4, and 8, so that the binary data stream has *n* equal to one symbol, two symbols, or three symbols for their respective messages. Thus, there are *M* signals with different frequencies to represent these *M* symbols.

3. M-Phase Shift Keying Modulation Scheme

Phase shift keying (PSK) was developed during the early days of the deep-space program. Now it is widely used in both military and commercial applications [10]. In PSK modulation, the phase of the carrier signal is shifted to represent data. In the simplest form of phase-shift keying, a pair of signals $s_1(t)$ and $s_2(t)$ are used to represent symbols 1 and 0, which are ninety degrees out of phase with each other. In this *binary phase shift keying* (BPSK), the signals are 180 degrees out of phase with each other. This can be accomplished by "flipping" the sine wave by multiplying one of the sinusoids by a negative one.

The bandwidth efficiency of the PSK modulation scheme is increased by using M-PSK modulation. Note that a more efficient use of bandwidth is achieved when each signaling element represents more than one bit. In BPSK, a single data bit (usually a high or a low voltage) is represented as a single symbol, either a 1 or a 0. In M-PSK, a single symbol is used to deal with $n = \log_2(M)$ data bits. However, increasing the bandwidth efficiency in this way usually increases the bit error rate. This thesis considers M-PSK modulation types where M = 2, 4, and 8, which corresponds to n = 1, 2, or 3 data bits. A M-PSK signal can be represented mathematically as

$$s_i(t) = A \cdot \cos\left(2\pi f_c t + \frac{2\pi}{M} i\right), \quad i = 1, 2, ..., M, \tag{2.2}$$

where A is the signal pulse shape, M is the number of possible phases of the carrier, and f_c is the carrier frequency. Figure 2 shows plots of the complex, polar-coordinate constellations for 2-PSK, 4-PSK, and 8-PSK modulation types. Many communications systems use this modulation type including satellite phones and global positioning systems. Quadrature phase-shift keying (QPSK is the same thing as 4-PSK) is currently used in applications such as cable modems and the

IS-95 (CDMA) system. It gives an illustration of the in-phase versus quadrature constellations of the various phase-shift keying modulation types used in this work.

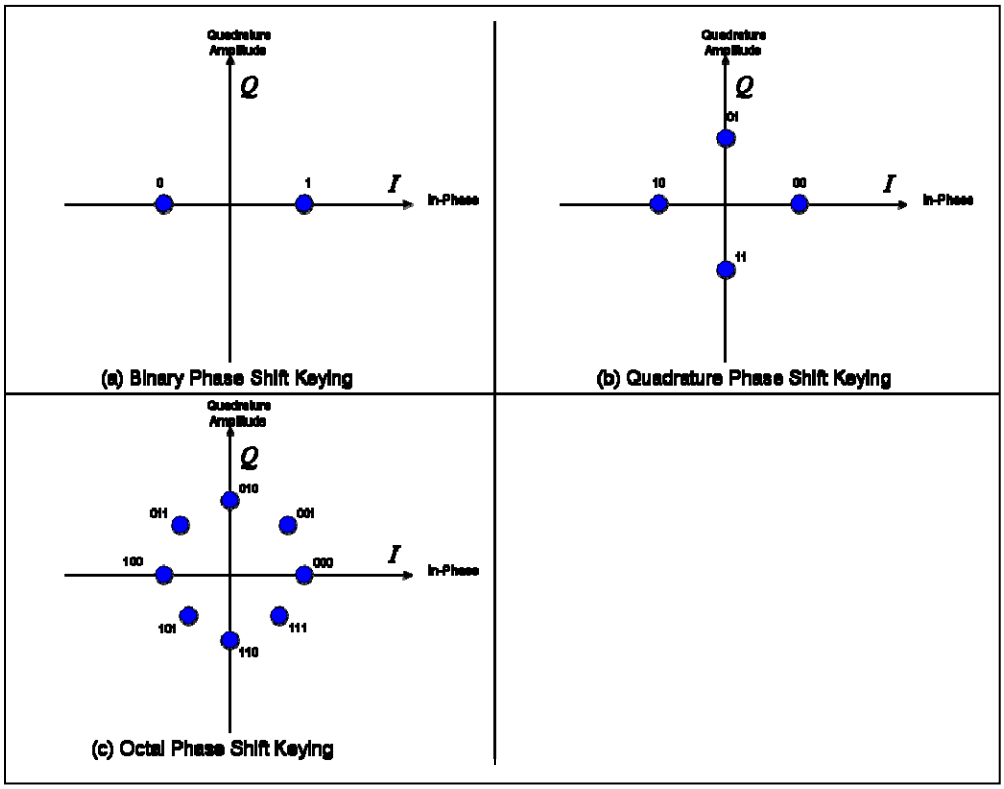

Figure 2. (a) 2-PSK, (b) 4-PSK, (c) 8-PSK Constellations

4. M-QAM Modulation Scheme

Both FSK and PSK modulation schemes are constant envelope schemes, which essentially means that the amplitude of the carrier wave remains constant (i.e., it *envelopes* the signal). Quadrature amplitude modulation (QAM) has a non-constant envelope, and thus the focus is more on bandwidth efficiency. QAM is widely used in modems designed for telephone communications [13], and is used in satellite systems, wireless networks, and mobile cell phone systems. This modulation technique, which combines PSK with ASK techniques, sends two different signals simultaneously on the same carrier frequency, by using two orthogonal copies of the carrier frequency. In this way, a binary 1 can be represented whenever a constant envelope carrier is present and a binary 0 is represented as the *absence* of a carrier wave. The two separate signals are then transmitted independently with the same carrier frequency by using two quadrature

carriers $\cos(2\pi f_c t)$ and $\sin(2\pi f_c t)$. These two separate modulated signals are then added and transmitted [1]. This structure of QAM allows for M discrete amplitude levels (M-QAM), and thus permits a symbol to contain more than one bit of information. The general form for an M-QAM signal is given by

$$s_i(t) = d_1(t)\cos(2\pi f_c t) - d_2(t)\sin(2\pi f_c t), \quad i = 1, 2, ..., M, \quad (2.3)$$

where $d_k(t)$ is the signal pulse shape along with the information bearing signal amplitudes of the quadrature carriers. The signal constellations for 16-QAM, 64-QAM, and 256-QAM are shown in Figure 3.

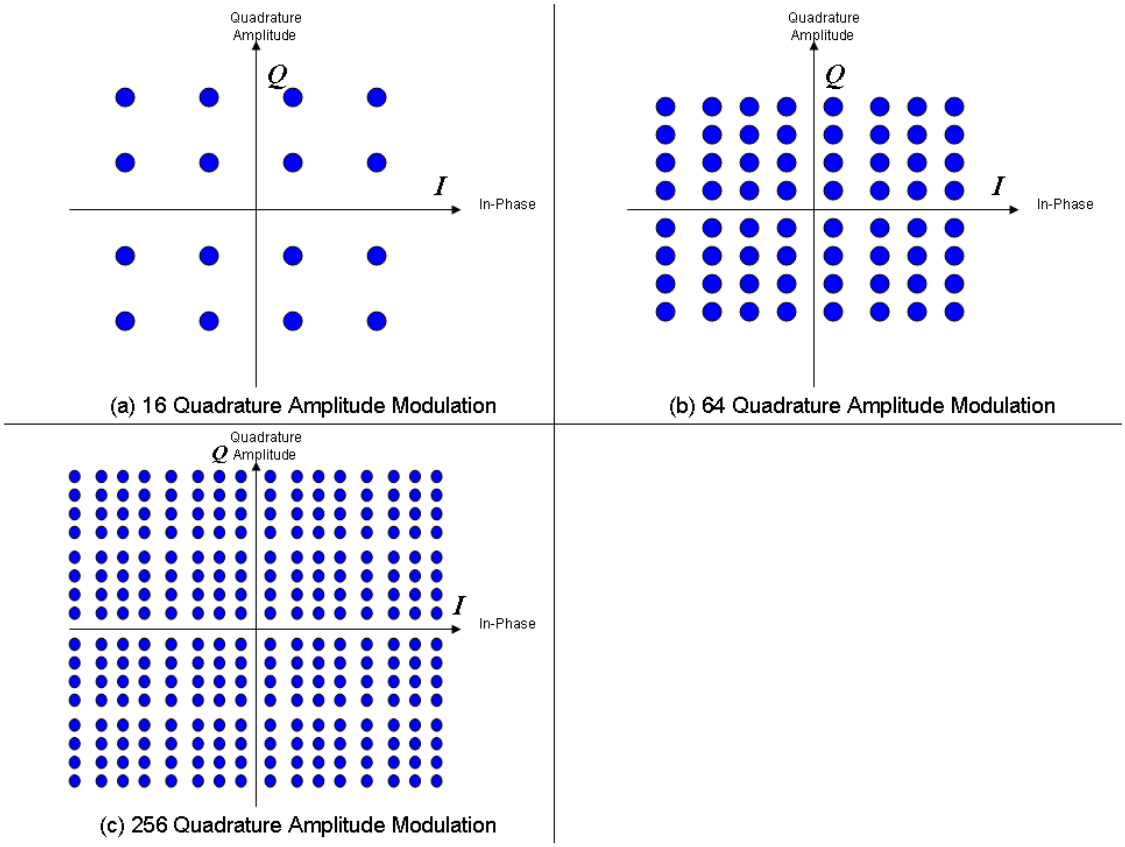

Figure 3. Signal Constellations for (a) 16-QAM, (b) 64-QAM, and (c) 256-QAM

THIS PAGE INTENTIONALLY LEFT BLANK

III. WIRELESS TRANSMISSION CHANNELS

This chapter introduces wireless transmission channels including additive white Gaussian noise and two types of multipath fading: Rayleigh fading and Ricean fading.

A. INTRODUCTION

Signals in a digital communication system must get from transmitter to receiver via a transmission channel, as depicted in Figure 1. A channel is therefore some kind of a physical medium that connects the transmitter and receiver. For analytical purposes, it is sometimes convenient to model the transmission channel as noiseless which means that the signal received is only the signal that was sent, nothing more and nothing less. However, communication channels introduce noise, fading, interference, and other distortions into the signals that they transmit. Simulating a communication system involves modeling a channel based on mathematical descriptions of the channel. Different transmission media have different properties and are therefore modeled differently. This chapter describes the channel features of additive white Gaussian noise and the two fading models; Ricean and Rayleigh fading.

B. ADDITIVE WHITE GAUSSIAN NOISE

The noise analysis of communication systems is often based on an idealized noise process called additive white Gaussian noise (AWGN). In this type of channel, the noise distorting our signal is a wide sense stationary random process that is independent of frequency. In fact, AWGN is defined in terms of its power spectral density which is given as

$$S_W(f) = \frac{N_0}{2}, \tag{3.1}$$

where N_0 is a constant and the factor $\frac{1}{2}$ has been included to indicated that half the power is associated with positive frequencies and half with negative frequencies. The

word *Gaussian* in the phrase additive white Gaussian noise is due to a Gaussian distribution of the amplitude of the noise (i.e., it has a normal "bell curve" distribution). AWGN leads to simple, tractable mathematical models useful for gaining insight into the underlying behavior of a system. Figure 4 shows the autocorrelation function and the power spectral density of white noise [15], [16].

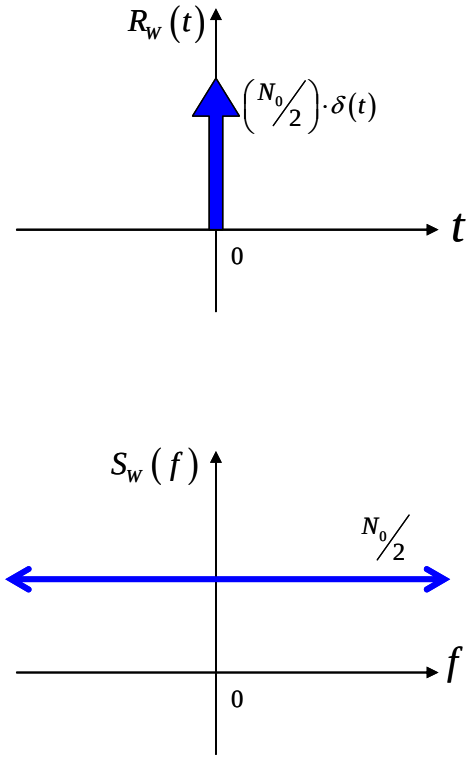

Figure 4. Autocorrelation function and the power spectral density of AWGN

C. FADING CHANNELS

When dealing with satellite and other communications systems where there is line of sight between the transmitter and receiver, the free-space propagation model gives simple theoretical explanations for propagation loss. However, with ground communications many obstructions can interfere with the transmission of a signal. Objects like mountains, buildings, densely wooded areas and rough terrain cause the signal to be reflected (i.e., bouncing off) and diffracted (i.e., bending around) these various surfaces in order to arrive at its destination. These obstacles cause signals to

scatter and these delayed versions to arrive at slightly different times. This phenomenon is known as multipath propagation and causes a phenomenon in real-world communications known as fading.

1. Rayleigh Distribution

In an environment where there are reflections off multiple local objects between the transmitter and receiver, rapid variations in the signal strength can occur. The reflections off the objects cause the phase of the carrier signal to change rapidly, which can sometimes add together destructively. This type of multipath fading channel is modeled with *Rayleigh fading*, which can be useful in modeling larger city environments where no lines of sight exist between the transmitter and receiver. Experimental work in Manhattan, New York has found near-Rayleigh fading there [17].

Statistically, the Rayleigh distribution is related to the central chi-square distribution and probability density function is defined as:

$$P_R(r) = \frac{r}{\sigma^2} e^{-r^2/2\sigma^2}, \quad \text{if} \quad r \geq 0, \tag{3.2}$$

where r models the power of each time delayed signal generated by the multipath distortion. If we assume a unit variance, then the probability density function curve looks as in Figure 5.

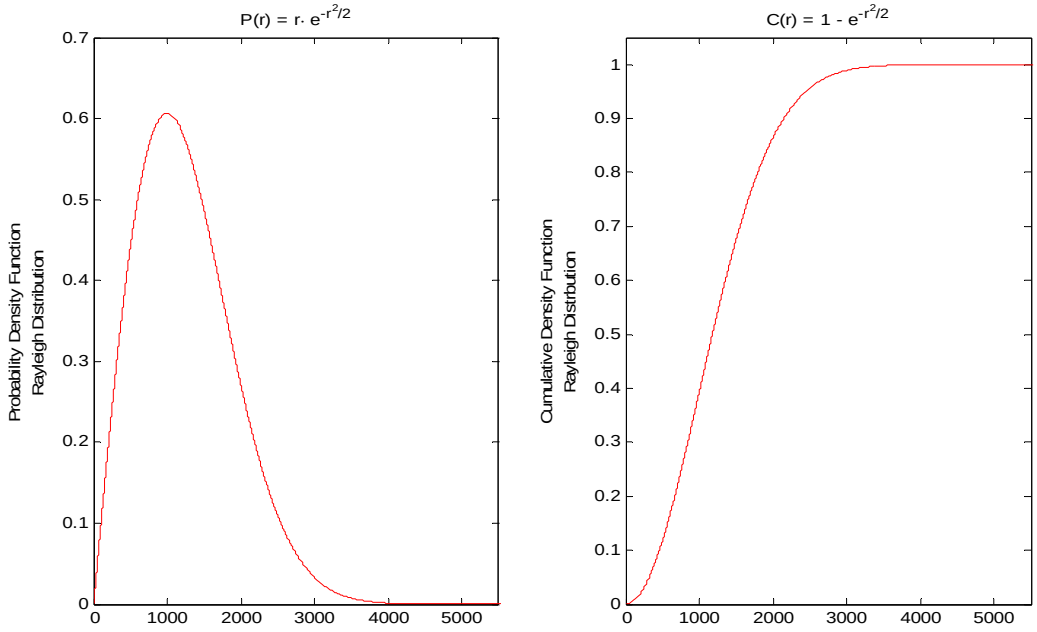

Figure 5. PDF and CDF of Rayleigh Distribution

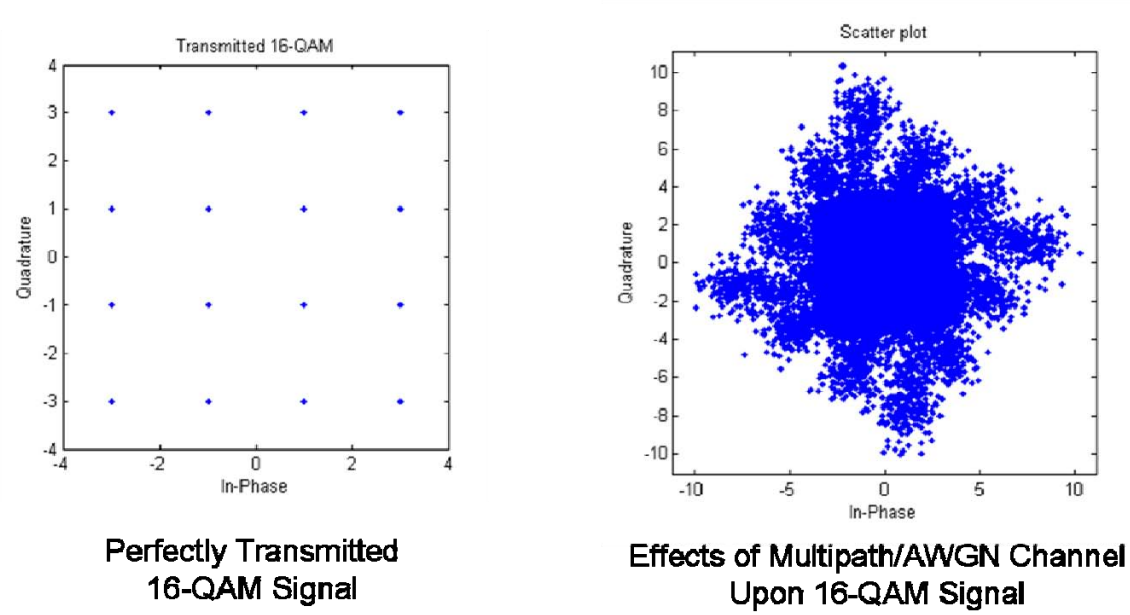

Figure 6. 256-QAM Constellation (Before and after transmission through AWGN and

2. Ricean Distribution

The *Ricean fading* model can be used to describe a multipath fading channel in which there is a line-of-sight (LOS) between the transmitter and the receiver, in addition to some of the scattering obstacles which cause fading. The line of sight signal corresponds to a strong, constant component to the signal. Thus, the Ricean fading model is simply a combination of the Rayleigh fading mentioned above *and* a line of sight component. The Ricean model could therefore be used whenever line of sight is reasonably available [18].

In the Rayleigh model above, the probability density function is closely related to the central chi-square distribution. In contrast, the Ricean model is related to the non-central chi-square distribution. The probability density function of this model is given in [19] as:

$$P_R(r) = \frac{r^{n/2}}{\sigma^2 s^{(n-2)/2}} e^{-\left(r^2+s^2\right)/2\sigma^2} \cdot I_{n/2-1}\left(\frac{rs}{\sigma^2}\right), \tag{3.3}$$

where the $I_{n/2-1}\left(\frac{rs}{\sigma^2}\right)$ is the $(n/2-1)$ order, modified Bessel function of the first kind, which may be represented using the infinite series representation

$$I_{n/2-1}\left(\frac{rs}{\sigma^2}\right) = \sum_{k=0}^{\infty} \frac{\left(\frac{1}{2}\cdot\frac{rs}{\sigma^2}\right)^{n/2-1+2k}}{k!\Gamma\left(n/2-1+k+1\right)}, \quad rs \geq 0. \tag{3.4}$$

Figure 7 shows the PDF and the CDF for the Ricean distribution, where the value for σ is determined by the standard deviation of the signal. This parameter is automatically detected and determined by the Simulink model developed in this thesis.

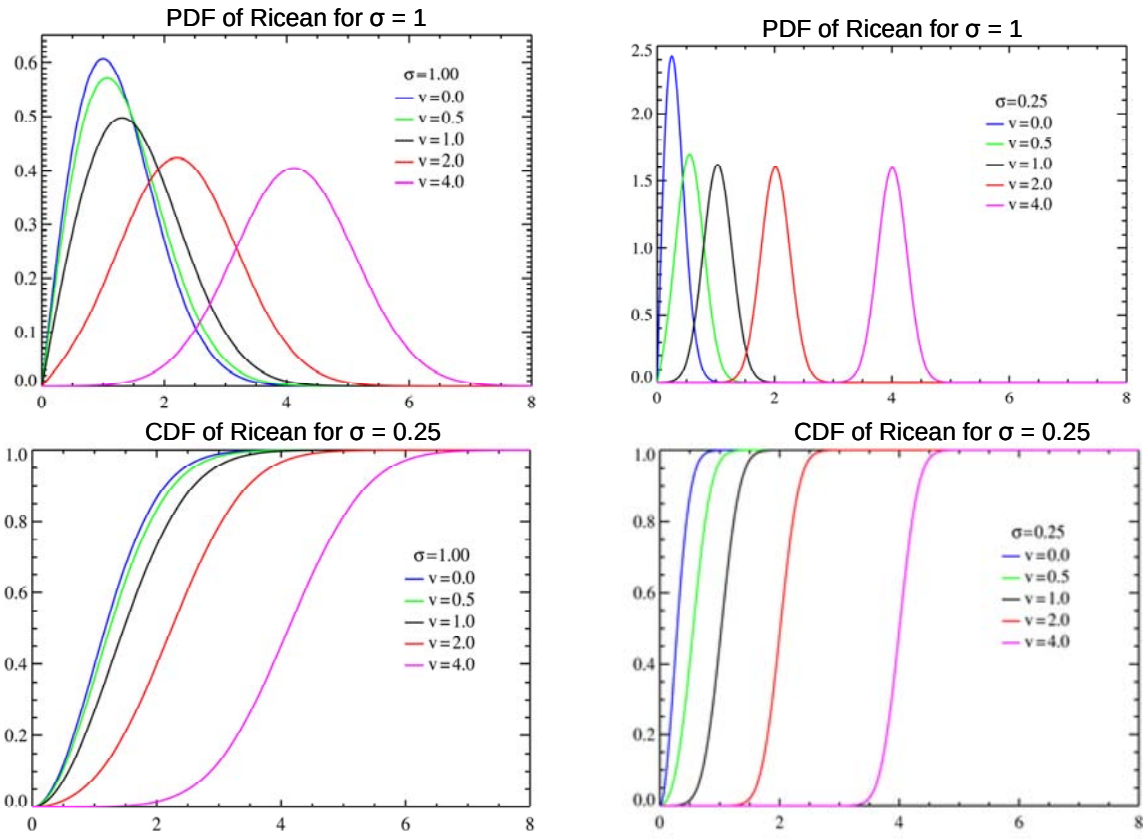

Figure 7. PDF and CDF of a Ricean Distribution

IV. MOMENTS AND CUMULANTS

This chapter discusses the higher order moments and cumulants which are the statistical features used to classify unknown modulation types.

A. INTRODUCTION

Moments and cumulants are statistical features used to help identify distinguishing characteristics of data. These statistical features have specifically been used in the field of signal processing to help identify the modulation type of a noisy signal [21]. The reason that moments and cumulants are used is that they are peculiarly resilient to noise effects. This thesis used these features, particularly second order to eighth order moments and cumulants to generate features used in the classification task.

B. MOMENTS

Moments are just a generalization of a common statistical average known as the mean, or the expected value of a dataset. In probability theory, the expected value of a discrete dataset is derived by taking each value in the dataset, multiplying it by the probability of that event occurring, and summing the resulting products. However, in Simulink, the Mean block tracks the mean values in a sequence of inputs over a period of time. Thus, if we let X be a discrete random variable then the moments of X are defined as

$$E_{x,a,b} = E\left[x^a \cdot \left(\bar{x}\right)^b \right], \text{ for } a,b \in \mathbb{Z}. \tag{4.1}$$

In the Simulink model, the expected value operator is approximated by a summation. Considering that all of the signals generated in this research are finite, the summation of course does not last forever. The summation will end at the last or n^{th} value and can be considered a "weighted average." The concept of the expected value described above gives way to application of calculating the moments of a random variable. Assuming that the mean of the signal being sent is zero, we then define the other central moments as simply powers of the random variable X. Thus the second order

moment is simply defined as $E\left\{X^2\right\}$. This moment describes the average signal power, simply because the value of X^2 is the power of the signal. Similarly, the m^{th} order moment is defined as $E\left\{X^m\right\}$. For the purposes of this research, the signal was simply raised to the corresponding power associated with the moment of interest to find the particular higher-order moment of the random signal, and then summed to produce the desired results.

C. CUMULANTS

Cumulants, like moments, are also statistical features of random variables. The moments described in section B above are used to ultimately define the cumulant. The cumulants are, more precisely, defined using the cumulant generating function, which is an extension of the moment generating function. According to [22], this cumulant generating function is defined as

$$g(t) = \log\left(E\left\{e^{tX}\right\}\right) = \sum_{n=1}^{\infty} \kappa_n \frac{t^n}{n!}. \tag{4.2}$$

Taking the derivatives of this expanded series, and then evaluating these derivatives at time $t = 0$ will lead to the κ_n values which correspond to the cumulants. Note that the first derivative of Equation 4.2 above gives the mean of the data being evaluated. The second derivative, gives the variance of the data being evaluated. Higher order cumulants also provide additional measures of central tendency of the data being evaluated.

Further, note that even ordered cumulants can be expressed as polynomials of equal or lower ordered moments [4]. This result made calculating cumulant quantities in Simulink far easier. For convenience, Table 2 lists the expressions for the cumulants up to order eight expressed in terms of the moment expressions, as reported in [4]. For every variation of the powers of the complex conjugate signal pairs, we have a different corresponding cumulant. These were the expressions used to generate the cumulants in this research. Thus, in the table below, the expression $C_{s,a,b}$ is meant to express the particular higher order cumulant of a complex signal, s, where a is the power of the

complex signal s and b is the power of the complex conjugate of s. Thus, when computing the cumulants from the moment generating function, the expectation operator will operate on the signal in the form:

$$s^a \cdot \left(\overline{s}\right)^b .$$

In summary, this chapter provides an overview of the statistical moments and cumulants used as the classification features in the modulation types to be detected.

Order	Cumulant	Expressed in terms of the Moments
2	$C_{s,2,0}$	$E_{s,2,0} = E\left[s^2 \cdot \left(\overline{s}\right)^0 \right]$ for $s \in \mathbb{C}$
2	$C_{s,1,1}$	$E_{s,1,1} = E\left[s \cdot \left(\overline{s}\right) \right]$
4	$C_{s,4,0}$	$E_{s,4,0} - 3 \cdot \left(E_{s,2,0}\right)^2$
4	$C_{s,3,1}$	$E_{s,3,1} - 3E_{2,0} \cdot E_{1,1}$
4	$C_{s,2,2}$	$E_{s,2,2} - \left(E_{s,2,0}\right)^2 - 2\left(E_{s,1,1}\right)^2$
6	$C_{s,6,0}$	$E_{s,6,0} - 15E_{s,2,0}E_{s,4,0} + 30\left(E_{s,2,0}\right)^3$
6	$C_{s,5,1}$	$E_{s,5,1} - 10E_{s,2,0}E_{s,3,1} - 5E_{s,1,1}E_{s,4,0} + 30\left(E_{s,2,0}\right)^2 E_{s,1,1}$
6	$C_{s,4,2}$	$E_{s,4,2} - E_{s,2,0}E_{s,4,0} - 8E_{s,1,1}E_{s,3,1} - 6E_{s,2,0}E_{s,2,2} + 6\left(E_{s,2,0}\right)^3 + 24\left(E_{s,1,1}\right)^2 E_{s,2,0}$
6	$C_{s,3,3}$	$E_{s,3,3} - 6E_{s,2,0}E_{s,3,1} - 9E_{s,1,1}E_{s,2,2} + 18\left(E_{s,2,0}\right)^2 E_{s,1,1} + 12\left(E_{s,1,1}\right)^3$
8	$C_{s,8,0}$	$E_{s,8,0} - 35\left(E_{s,4,0}\right)^2 - 630\left(E_{s,2,0}\right)^4 + 420\left(E_{s,2,0}\right)^2 E_{s,4,0}$
8	$C_{s,7,1}$	$E_{s,7,1} - 35E_{s,4,0}E_{s,3,1} - 630\left(E_{s,2,0}\right)^3 E_{s,1,1} + 210E_{s,4,0}E_{s,2,0}E_{s,1,1} + 210E_{s,2,0}E_{s,3,1}$
8	$C_{s,6,2}$	$E_{s,6,2} - 15E_{s,4,0}E_{s,2,2} - 20\left(E_{s,3,1}\right)^2 + 30E_{s,4,0}\left(E_{s,2,0}\right)^2 + 60E_{s,4,0}\left(E_{s,1,1}\right)^2$ $+240E_{s,3,1}E_{s,1,1}E_{s,2,0} + 90E_{s,2,2}\left(E_{s,2,0}\right)^2 - 90\left(E_{s,2,0}\right)^4 - 540\left(E_{s,2,0}\right)^2\left(E_{s,1,1}\right)^2$
8	$C_{s,5,3}$	$E_{s,5,3} - 5E_{s,4,0}E_{s,3,1} - 30E_{s,3,1}E_{s,2,2} + 90E_{s,3,1}\left(E_{s,2,0}\right)^2 + 120E_{s,3,1}\left(E_{s,1,1}\right)^2$ $+180E_{s,2,2}E_{s,1,1}E_{s,2,0} + 30E_{s,4,0}E_{s,2,0}E_{s,1,1} - 270\left(E_{s,2,0}\right)^3 E_{s,1,1} - 360\left(E_{s,1,1}\right)^3 E_{s,2,0}$
8	$C_{s,4,4}$	$E_{s,4,4} - \left(E_{s,4,0}\right)^2 - 18\left(E_{s,2,2}\right)^2 - 16\left(E_{s,3,1}\right)^2 - 54\left(E_{s,2,0}\right)^4 - 144\left(E_{s,1,1}\right)^4 - 432\left(E_{s,2,0}\right)^2\left(E_{s,1,1}\right)^2$ $+12E_{s,4,0}\left(E_{s,2,0}\right)^2 + 96E_{s,3,1}E_{s,1,1}E_{s,2,0} + 144E_{s,2,2}\left(E_{s,1,1}\right)^2 + 72E_{s,2,2}\left(E_{s,2,0}\right)^2 + 96E_{s,3,1}E_{s,2,0}E_{s,1,1}$

Table 2. Higher Order Cumulants Expressed as Polynomials of Moments

D. FEATURE EXTRACTION OF SIGNALS

Two Simulink models were implemented in this work; the first one was used to derive the signals while the second computed the signal's statistical features following the results discussed in Chapter V. Figure 8 illustrates the blocks used to compute the fourth-order moment. First, the signal was raised to the power of the desired moment. Next, the arithmetic mean block was applied (along with the option for computing the running mean checked) to derive the expected value.

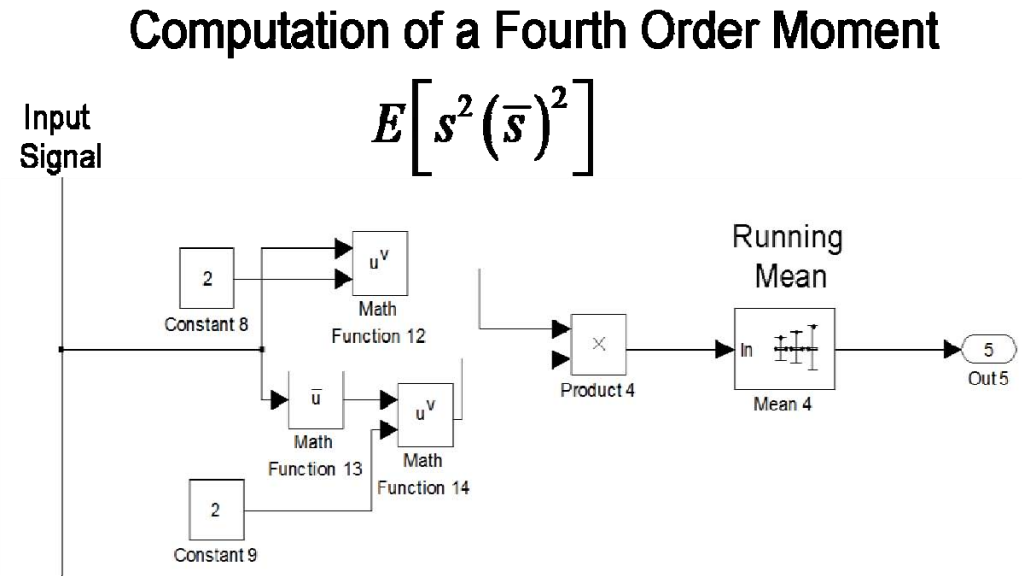

Figure 8. 4th Order Moment Simulink Block

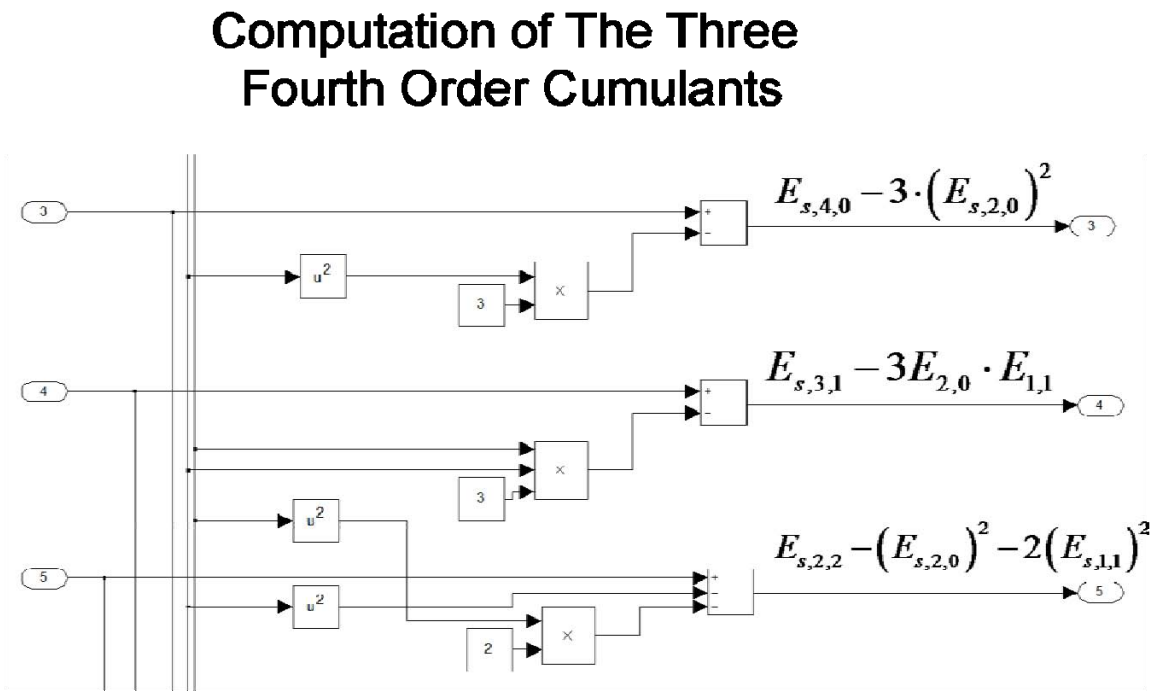

Figure 9. 4th Order Cumulants Simulink block

Figure 9 illustrates the Simulink-based blocks used in the derivation of the fourth-order cumulant quantity. In this case, the inputs to the cumulant-generating model are the outputs of the moment-generating model. The results of these features are provided in Table 3 for the signals without any noise, and also in Table 4 for the signals with noise at the SNR level of 5dB (i.e., very noisy AWGN) for comparison.

	BPSK	4-PSK	8-PSK	2-FSK	4-FSK	8-FSK	16-QAM	64-QAM	256-QAM
SNR	∞	∞	∞	∞	∞	∞	∞	∞	∞
E_s20	1.00	0.00	0.00	1.00	1.00	1.00	0.00	0.00	0.00
E_s11	1.00	1.00	1.00	1.00	1.00	1.00	1.00	1.00	1.00
E_s40	1.00	1.00	0.00	1.00	1.00	1.00	-0.69	-0.60	-0.60
E_s31	1.00	0.00	0.00	0.00	0.00	0.00	0.00	0.00	0.00
E_s22	1.00	1.00	1.00	1.00	1.00	1.00	1.32	1.37	1.40
E_s60	1.00	0.00	0.00	0.00	0.00	0.00	0.00	0.00	0.00
E_s51	1.00	1.00	0.00	0.00	0.00	0.00	-1.33	-1.25	-1.27
E_s42	1.00	0.00	0.00	0.00	0.00	0.00	0.00	0.00	0.00
E_s33	1.00	1.00	1.00	1.00	1.00	1.00	1.96	2.19	2.29
E_s80	1.00	1.00	1.00	0.00	0.00	0.00	2.22	1.80	1.77
E_s71	1.00	0.00	0.00	0.00	0.00	0.00	0.00	0.00	0.00
E_s62	1.00	1.00	0.00	0.00	0.00	0.00	-2.50	-2.66	-2.76
E_s53	1.00	0.00	0.00	0.00	0.00	0.00	0.00	0.00	0.00
E_s44	1.00	1.00	1.00	1.00	1.00	1.00	3.13	3.87	4.17
C_s20	1.00	0.00	0.00	0.00	0.00	0.00	0.00	0.00	0.00
C_s11	1.00	1.00	1.00	1.00	1.00	1.00	1.00	1.00	1.00
C_s40	-2.00	1.00	0.00	0.00	0.00	0.00	-0.69	-0.60	-0.60
C_s31	-2.00	0.00	0.00	0.00	0.00	0.00	0.00	0.00	0.00
C_s22	-2.00	-1.00	-1.00	-1.00	-1.00	-1.00	-0.69	-0.60	-0.60
C_s60	16.00	0.00	0.00	0.00	0.00	0.00	0.00	0.00	0.00
C_s51	16.00	-4.00	0.00	0.00	0.00	0.00	2.10	1.75	1.73
C_s42	16.00	0.00	0.00	0.00	0.00	0.00	0.00	0.00	0.00
C_s33	16.00	4.00	4.00	4.00	4.00	4.00	2.10	1.75	1.79
C_s80	-244.00	-34.00	1.00	0.00	0.00	0.00	-14.56	-10.85	-10.71
C_s71	-244.00	0.00	0.00	0.00	0.00	0.00	0.00	0.00	0.00
C_s62	-244.00	46.00	0.00	0.00	0.00	0.00	-30.51	-26.26	-26.38
C_s53	-244.00	0.00	0.00	0.00	0.00	0.00	0.00	0.00	0.00
C_s44	-244.00	-18.00	-17.00	-17.00	-17.00	-17.00	17.30	23.20	25.41

Table 3. Moments and Cumulants without Disturbance (SNR = ∞)

	BPSK	4-PSK	8-PSK	2-FSK	4-FSK	8-FSK	16-QAM	64-QAM	256-QAM
SNR	5	5	5	5	5	5	5	5	5
E_s20	0.76	0.01	0.02	0.76	0.76	0.76	-0.01	0.01	-0.03
E_s11	1.00	0.99	0.99	1.00	1.00	1.00	0.99	1.00	0.98
E_s40	0.59	0.60	0.01	0.56	0.58	0.57	-0.27	-0.23	-0.17
E_s31	1.13	0.04	0.06	1.13	1.13	1.12	-0.04	0.02	-0.06
E_s22	1.43	1.40	1.43	1.44	1.43	1.42	1.72	1.77	1.75
E_s60	0.49	0.07	0.03	0.42	0.40	0.47	0.23	0.05	0.06
E_s51	1.17	1.20	0.00	1.10	1.12	1.15	-0.95	-0.75	-0.60
E_s42	2.10	0.12	0.15	2.10	2.10	2.07	-0.17	0.04	-0.15
E_s33	2.55	2.52	2.62	2.60	2.57	2.57	4.31	4.46	4.37
E_s80	0.48	0.40	0.33	0.49	0.11	0.45	0.55	0.78	-0.50
E_s71	1.23	0.21	0.12	1.01	0.88	1.21	1.89	0.29	0.33
E_s62	2.71	2.74	-0.16	2.49	2.51	2.69	-4.26	-2.96	-2.46
E_s53	4.57	0.36	0.39	4.60	4.57	4.61	-0.83	0.32	-0.48
E_s44	5.49	5.40	5.86	5.65	5.58	5.58	13.85	14.32	13.82
C_s20	0.76	0.01	0.02	0.76	0.76	0.76	-0.01	0.01	-0.03
C_s11	1.00	1.00	1.00	1.01	1.00	1.00	1.00	1.00	0.98
C_s40	-1.14	0.60	0.00	-1.15	-1.16	-1.13	-0.27	-0.22	-0.17
C_s31	-1.15	0.01	0.01	-1.15	-1.15	-1.14	0.00	0.00	0.03
C_s22	-1.16	-0.57	-0.55	-1.15	-1.15	-1.14	-0.24	-0.20	-0.18
C_s60	6.98	-0.03	0.03	7.07	7.11	6.92	0.21	0.07	0.04
C_s51	7.02	-1.79	-0.04	7.04	7.07	6.92	0.38	0.38	0.26
C_s42	7.04	-0.03	-0.03	7.04	7.06	6.92	-0.01	-0.02	-0.08
C_s33	7.05	1.74	1.68	7.04	7.06	6.92	0.49	0.39	0.26
C_s80	-79.78	-12.02	0.34	-82.55	-83.93	-78.69	-1.94	-1.21	-1.54
C_s71	-68.95	0.90	0.18	-69.05	-71.60	-66.89	2.42	-0.22	0.97
C_s62	-52.91	25.74	0.00	-53.87	-53.61	-51.33	-13.28	-10.25	-7.92
C_s53	-37.88	2.08	3.13	-37.27	-37.33	-35.74	-3.06	1.90	-3.19
C_s44	-31.36	28.92	31.56	-30.00	-30.42	-28.98	66.89	69.25	67.64

Table 4. Moments and Cumulants with SNR = 5 dB

V. ORGANIZATION OF MATLAB AND SIMULINK MODELING SOFTWARE

This chapter describes the software implementation of the MATLAB code and Simulink models used to classify the digital signals.

A. THE CLASSIFICATION TREE

The essential heart of this thesis is the classification tree. This system takes an unknown signal, with a randomly generated level of noise, and uses higher order statistical moments and cumulants to make threshold decisions. If the statistical feature of the noisy, multipath signal does not meet the threshold criteria, then the signal does not belong to the modulation types associated with that feature. If, on the other hand, the statistical feature does meet the threshold criteria, then the classifier decides that only certain (or one) modulation type can correspond to these criteria.

How were the statistical features chosen, so that the classification tree works correctly? First, the statistical data was placed in a Microsoft Excel spreadsheet showing the 28 different moments and cumulants matched with the modulation types. The data was collected for both very high and very low signal to noise ratios. This data is provided in the two tables below. Note that the two tables only show values of the moments and cumulants for an SNR level of 5dB and infinite SNR. However, this is only for convenience. Tables of course could be made for all SNR levels, say between 0dB and 100dB, but one hundred charts would be too much information. These tables with two values (low and high) are chosen for quick understanding of the effects of high levels of noise on the higher order statistics of interest.

STATISTICAL CRITERIA									
	BPSK	**4PSK**	**8PSK**	**2FSK**	**4FSK**	**8FSK**	**16QAM**	**64QAM**	**256QAM**
Eb/N0	inf	inf	inf	inf	inf	inf	inf	inf	inf
mom20	1	0	0	0	0	0	0	0	0
mom11	1	1	1	1	1	1	0.765108	0.989302	0.998138
mom40	1	1	0	0	0	0	-0.68	-0.62	-0.61538
mom31	1	0	0	0	0	0	0	0	0
mom22	1	1	1	1	1	1	1.307515	1.352082	1.394862
mom60	1	0	0	0	0	0	0	0	0
mom51	1	1	0	0	0	0	-1.27997	-1.2326	-1.31684
mom42	1	0	0	0	0	0	0	0	0
mom33	1	1	1	1	1	1	1.919948	2.138177	2.257448
mom80	1	1	1	0	0	0	2.092815	1.755001	1.851187
mom71	1	0	0	0	0	0	0	0	0
mom62	1	1	0	0	0	0	2.406737	-2.574	-2.85183
mom53	1	0	0	0	0	0	0	0	0
mom44	1	1	1	1	1	1	3.034582	3.802503	4.252727
qum20	1	0	0	0	0	0	0	0	0
qum11	1	1	1	1	1	1	1	1	1
qum40	-2	1	0	0	0	0	-0.68902	-0.61925	-0.59416
qum31	-2	0	0	0	0	0	0	0	0
qum22	-2	-1	-1	-1	-1	-1	-0.67931	-0.62737	-0.60123
qum60	16	0	0	0	0	0	0	0	0
qum51	16	-4	0	0	0	0	2.094489	1.760851	1.693086
qum42	16	0	0	0	0	0	0	0	0
qum33	16	4	4	4	4	4	2.065399	1.823739	1.73071
qum80	-244	-34	1	0	0	0	-14.4404	-11.4075	-10.5067
qum71	-244	0	0	0	0	0	0	0	0
qum62	-244	46	0	0	0	0	-30.3458	-27.2025	-26.0167
qum53	-244	0	0	0	0	0	0	0	0
qum44	-244	-18	-17	-17	-17	-17	17.68429	23.98502	25.51636

Table 5. Higher Order Statistics for High SNR Levels (i.e., Eb/N0 = ∞)

STATISTICAL CRITERIA									
Eb/N0	5	5	5	5	5	5	5	5	5
mom20	0.7600	0	0	0.0000	0.0000	0.0000	0	0	0
mom11	1	1	1	1	1	1	1	1	1
mom40	0.5800	0.5700	0.018	-0.0200	-0.0100	-0.1000	-0.2700	-0.2000	-0.1500
mom31	1.125	-0.01	0	-0.02	-0.01	0.04	0	0	-0.01
mom22	1.42	1.42	1.42	2	2	2	1.7	1.8	1.8
mom60	0.45	0.047	-0.04	0.06	-0.4	0.14	-0.0601	-0.007	0.06
mom51	1.14	1.15	0.04	-0.01	0.07	-0.6	-0.85	-0.65	-0.55
mom42	2.07	-0.02	0.01	-0.01	-0.07	0.2	0	0.01	-0.06
mom33	2.56	2.56	2.56	5.7	5.8	6	4.1	4.56	4.63
mom80	0.33	0.45	0.44	-1	-1.2	0.5	0.6	-0.1	0
mom71	1.1	0.1	-0.05	0.3	-2.8	1	-0.3	0	0.16
mom62	2.63	2.67	0.15	-1	1	-4.4	-3.01	-2.5	-2.1
mom53	4.56	-0.07	0.04	-1	0	0.9	-0.1	0.1	-0.2
mom44	5.5	5.5	5.5	22	23	24.5	12	14.5	15
qum20	0.76	0	0	0	0	0	0	0	0
qum11	1	1	1	1	1	1	1	1	1
qum40	-1.15	0.6	0	-0.02	-0.01	-0.1	-0.27	-0.19	-0.16
qum31	-1.15	0	0	-0.01	0	0	0	0	0
qum22	-1.15	-0.56	-0.57	-0.03	-0.02	0	-0.27	-0.19	-0.17
qum60	7	0.03	0	0.06	-0.4	0.16	-0.05	0	0.03
qum51	7	-1.75	-0.03	-0.02	0.1	-0.08	0.53	0.33	0.26
qum42	7	0	0	-0.02	0.02	0	0	0	0.01
qum33	7	1.75	1.75	0.04	0.02	0.08	0.53	0.3	0.3
qum80	-80	-11.5	0.53	-1	-1.1	0	-2	-1.44	-1
qum71	-68	0.05	-0.05	0.5	-2.8	1	-0.43	0	0.2
qum62	-53	25	0.75	-1.1	0.7	-7.5	-12.5	-9	-7.3
qum53	-38	-0.2	0.25	-3.3	-1.2	3.5	0.121	0.27	-1
qum44	-31	30	30	90	94	95	63	72	73

Table 6. Higher Order Statistics for Low SNR Level (i.e., Eb/N0 = 5dB)

Using Microsoft Excel, and importing these values into MATLAB, allowed a reasonable analysis of the data using a surface plot. The surface plot clearly shows that some values of the higher order statistics are significantly different than the others, which in turn clearly distinguishes specific modulation types from other ones. This distinguishing feature remains present, even in very high levels of noise. Figure 10 and Figure 11 show two surface plots, clearly showing unique features in the entire collection of higher order statistics.

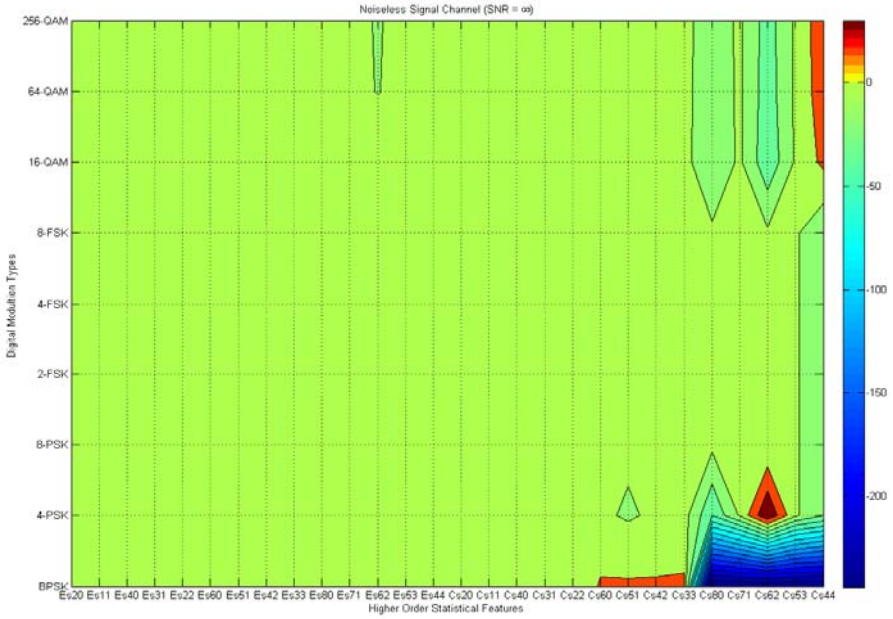

Figure 10. Surface Plot of Higher Order Statistics Against All Modulation Types Under Noiseless Conditions (SNR = ∞)

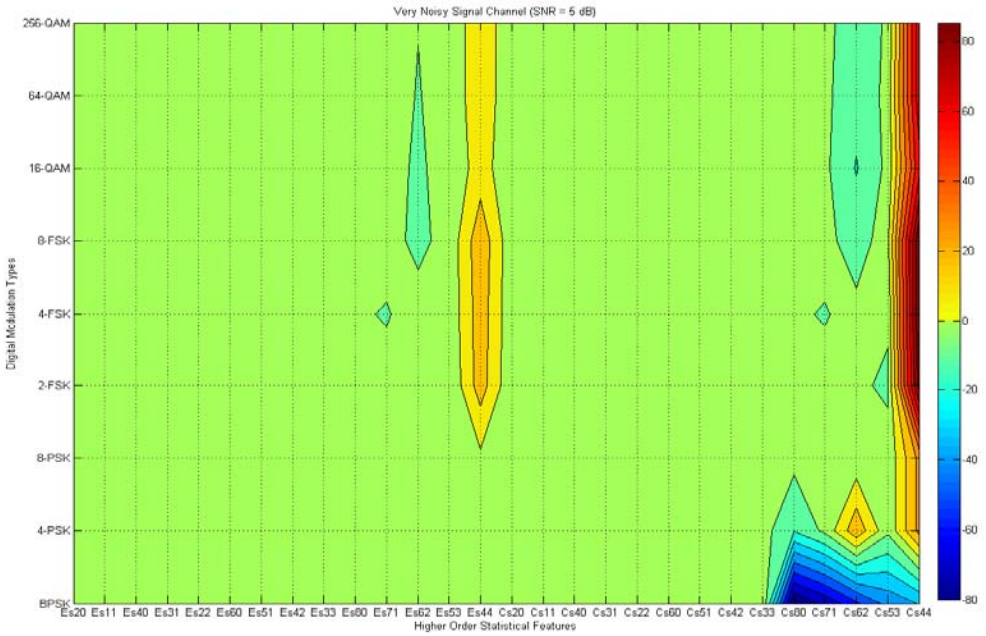

Figure 11. Surface Plot of Higher Order Statistics Against All Modulation Types Under Extremely Noisy Conditions (SNR = 5dB)

In Figure 10 and 11, it can be seen that the most significantly different values fall along the binary phase shift keying, corresponding to the eighth order cumulants. Also, this feature (the blue areas in the figures) remains consistent despite the noise levels. Thus the classification program simply looks for these values and chooses the guess of BPSK if these eighth order cumulants fall below a reasonable threshold of this. However, if this threshold is not met, then the classification program continues, displaying to the user that – so far – it deduces that the signal must be any of the remaining modulation types: 4PSK, 8PSK, M-FSK or M-QAM. The classification tree continues on in this manner until the correct modulation type is guessed. A diagram of this classification tree is provided in Figure 12 below, for user convenience.

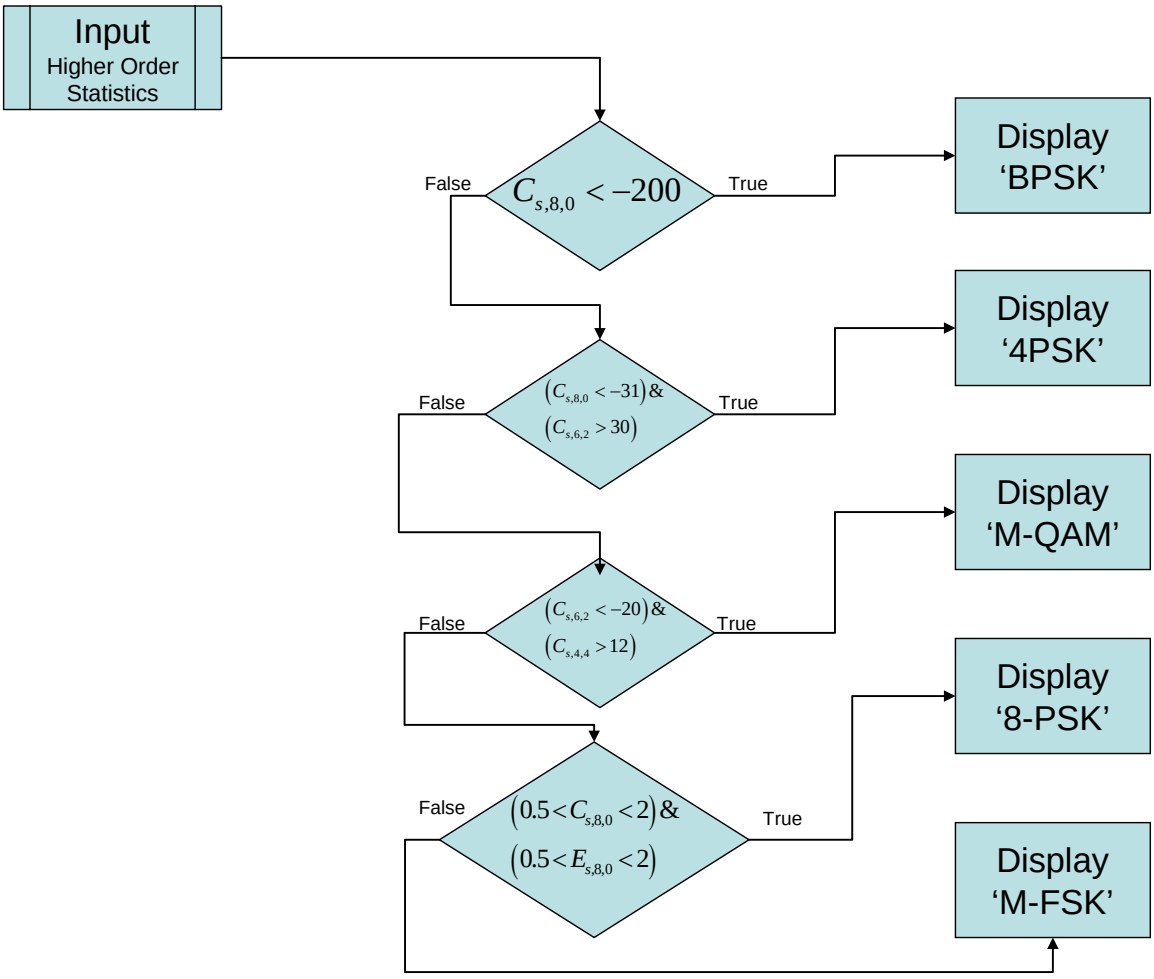

Figure 12. Diagram of Classification Tree

B. SOFTWARE IMPLEMENTATION

To start the program, the MATLAB file *CLASSIFIER.m* must be opened and run from the MATLAB Current Directory. This opens a dialogue for the user to read at the Command Window. The dialogue prompts the user to choose one of five options. These options allow the user to 1) generate a new signal for detection, 2) choose a modulation type to detect, 3) compute the higher order statistical features, and 4) allows the user to run the classification tree program. Finally, option 5) allows the user to simply quit, which exits the program.

The MATLAB m-file *CLASSIFIER.m* will, when prompted, will access, open and run the Simulink model for the signals, generating the statistical features to be trained. Finally, the classification program, which actually classifies the statistical features, will decide for the user what the previously unknown signal was.

Finally, it is very instructive, both for understanding the flow of the programming as well as debugging of the MATLAB code, to have a diagrammatic flow chart. This chart begins with an input signal, generated in Simulink. The outputs of the Simulink model move to the workspace in MATLAB. These variables are then called in an m-file which chooses a single signal (or all of them if slightly modified). This signal is then propagated through a noisy channel. This noisy signal is then sent to another Simulink model, which computes all the higher order statistics. These moments and cumulants are then brought back into another m-file to be normalized according to the output powers (after disturbances have been applied). These normalized moments and cumulants are then plugged into the classification tree shown in Figure 12. This overall program diagram is shown in Figure 13 below.

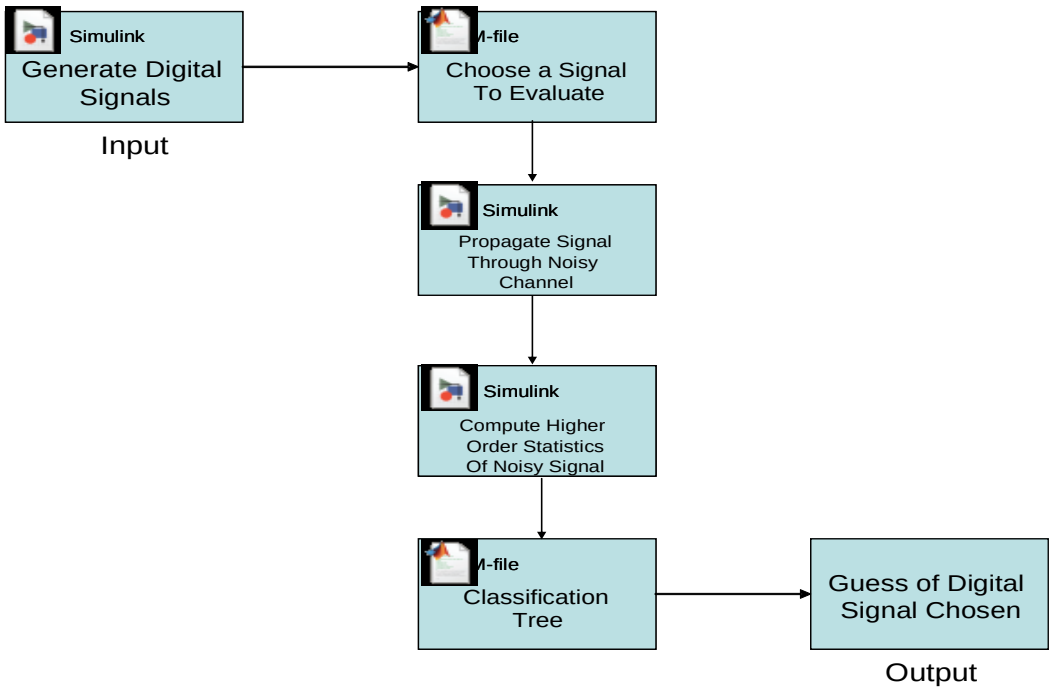

Figure 13. Overall Flowchart of MATLAB and Simulink Program

THIS PAGE INTENTIONALLY LEFT BLANK

VI. SIMULATION RESULTS

There were several assumptions made and features tested in order to arrive at the results found in this research. The first assumption was that the signals were zero mean. This proves to be true in all the signal generation tests run. The zero mean assumption was utilized because this greatly facilitates the mathematical equations associated with calculating higher order statistics. The second assumption was a simulation time of 20,000 seconds, which corresponds to generating signal arrays that are saved as 1×20000 vectors in MATLAB's workspace. Note that simulation time is not the same as clock time on the computer. The amount of time it takes to run a simulation depends on many factors, including the model's complexity, the solver's step sizes, and the computer's speed. The simulation time value can be changed in the configuration parameters of Simulink. This provided enough data to grab accurate approximations of the statistical features that correctly match the theoretical values on all nine of the signal modulation types. Each signal modulation type was tested 100 times in the classification algorithm to derive statistics for the results. Finally, each signal modulation type was sent through three different channels including AWGN, Rayleigh fading, and Ricean fading. These three channels in turn were tested in various levels of noise from no noise (i.e., for $E_b / N_0 = 100$, or essentially noiseless) to extreme noisy conditions (i.e., for $E_b / N_0 = 0$). Appendices A, B, C, and D provide the precise details of how this program works and how the statistical features were generated.

A. CLASSIFICATION RESULTS - ARBITRARY SIGNAL CHOICE

The first series of experiments assumed that the signal-to-noise ratio had a randomly chosen integer value between zero and 100 decibels. Additionally, the signal to be detected in this random noise level was also chosen at random. Thus, choice of the signal was determined by a numeric value between zero and eight. The table below shows these choices.

Choice	Signal Modulation Type
0	Binary Phase Shift Keying
1	4ary Phase Shift Keying
2	8ary Phase Shift Keying
3	2ary Frequency Shift Keying
4	4ary Frequency Shift Keying
5	8ary Frequency Shift Keying
6	16 Quadrature Amplitude Modulation
7	64 Quadrature Amplitude Modulation
8	256 Quadrature Amplitude Modulation

Table 7. Choice Value Associated with Signal Modulation Types

The program was run 100 times and the results were collected. When the classifier came to a conclusion about the type of signal that it received, a decision value was assigned that, like the choice above, had a value between zero and eight. If the choice and decision had the same value, then the current element of the results vector was assigned the value one, to represent a correct guess to the randomly chosen modulation type. However, if the decision and choice values were not the same, then the current element of the results vector was assigned a zero, representing an incorrect answer. Using these features, and considering all fading conditions, it was determined that the classifier was correct for a randomly sent signal under randomly high or low SNR levels (low: 0dB to 8dB; high: 50dB to 100dB) over 83.9% of the time. This value was determined by the average of all overall classification rates. The value of 83.9% was obtained by first allowing the program to randomly choose one of nine different modulation types. The SNR level was also randomly generated as an integer value between 0dB and 8dB for noisier conditions and 50dB to 100dB for less noisy conditions. If the true signal was modulated via 2, 4, or 8-PSK, under all noise and fading conditions, the classification scheme was correct 87.8% of the time. If the signal generated was any of the FSK modulation types, the classifier would correctly identify the signal as M-FSK

(with no additional specification) 84.5% of the time. If the signal generated was 16 or 64-QAM, the general case of the M-QAM signal type (i.e., either 16- or 64-QAM) can be correctly classified 77.8% of the time under all noise and fading conditions, as reflected in the average of M-QAM modulation types in Tables 8 through 13. The 256-QAM signal type, under all noise and fading conditions can be correctly identified 78.2% of the time for randomly chosen high or low SNR levels and 100 trials as reflected as the average of the 256-QAM types.

B. CLASSIFIER RESULTS: M-PSK SIGNALS

M-ary phase shift keying (M-PSK) modulated signals had the greatest levels of success when intentionally chosen. This means that the user must remove the code generating a random choice for the signal modulation types and replace it with a choice of zero, one, or two, as tabulated in Table 7 above. When this is done, and the program is run through 100 trials, with all randomly chosen SNR levels and all fading conditions, the results vector described above resulted in an 87.8% success rate in correct detection. This value was obtained by taking the average of the overall classification rates for PSK type signals from Tables 8 through 13. This result assumes that the classifier is totally unaware of the input SNR level, which would be expected in a real-world environment. The receiver cannot "know" ahead of time the level of noise present in the signal it is about to receive.

When tests were run on specifically higher SNR levels (i.e., randomly chosen between 50dB and 100dB), and no fading, the ability to successfully classify M-PSK was increased to 99% as can be seen in Table 8. When tests were run on specifically lower SNR levels (i.e., randomly chosen between 0dB and 8dB) and no fading, the ability to successfully classify M-PSK was reduced to 79%, as shown in Table 9. Under Rayleigh fading conditions, and low noise (SNR range: 50dB to 100dB), the success rate for M-PSK signals is over 99%, as can be seen in Table 10. For Rayleigh fading conditions and high noise (SNR range: 0dB to 8dB), the success rate is reduced to 77%, which is reflected in Table 11. For Ricean fading conditions, and low noise (SNR range: 50dB to 100dB), the success rate is 96%, as shown in Table 12. Finally, for Ricean fading conditions and high noise (SNR range: 0dB to 8dB), the success rate is reduced to 74% as

can be seen in Table 13. These percentages were acquired by taking the arithmetic mean of the first three values in the main diagonal of the confusion matrix, corresponding to BPSK, 4-PSK, and 8-PSK respectively.

B. CLASSIFIER RESULTS - M-FSK SIGNALS

The higher order statistics for the M-ary frequency shift keying (M-FSK) modulation types are impossible to distinguish from one another using the statistical features studied in this research. The reason for this is that the three types of FSK signals tested (i.e., M = 2, 4, and 8) all have almost the exact the same higher order moments and cumulants. Thus, the program, which seeks to find distinguishing differences in higher order statistical moments and cumulants, cannot distinguish between the different FSK types. However, if the program is run in an attempt to identify the M-FSK family *in general*, then the program is able to correctly identify it as such 84.5% of the time for all noise levels and all fading conditions. This value was obtained by taking the average of all M-FSK values on the main diagonals of Tables 8 through 13.

Thus, for randomly chosen higher SNR levels (SNR range: 50dB to 100dB) and no fading, the user specifically chooses one of the three types of M-FSK signals to pass through the classifier. After the higher order statistics are established, the classifier can correctly determine that the signal sent was M-FSK (and no additional specificity) 98% of the time, for 100 trials, which is indicated in Table 8. When tests were run on specifically lower SNR levels (i.e., randomly chosen between 0dB and 8dB), the ability to successfully classify M-FSK signals were reduced to 81%, as indicated in Table 9. When the tests were run on specifically higher SNR levels (i.e., randomly chosen between 50dB and 100dB), the ability to successfully classify M-FSK was increased to 98%. Under Rayleigh fading conditions, and low noise (SNR range: 50dB to 100dB), the success rate for M-FSK signals is over 98%, as indicated in Table 10. For Rayleigh fading conditions and high noise (SNR range: 0dB to 8dB), the success rate is reduced to 65%, which is reflected in Table 11. For Ricean fading conditions, and low noise (SNR

range: 50dB to 100dB), the success rate is 98%, as seen in Table 12. Finally, for Ricean fading conditions and high noise (SNR range: 0dB to 8dB), the success rate is reduced to 67%, which is reflected in Table 13.

C. CLASSIFIER RESULTS: M-QAM SIGNALS

The higher order statistics for the M-ary QAM signals are easier to distinguish than the FSK signals, but there are still some difficulties. While the 256-QAM signals can be differentiated from the 16 or 64-QAM signals, it remains that the 16- and 64-QAM signal types are again, very difficult to distinguish from each other using higher order statistics only. This limitation results from the fact that the features selected for the classification task are essentially identical for the 16- and 64-QAM types. This being said, the general case of the M-QAM signal type (i.e., either 16- or 64-QAM) can be correctly classified 77.8% of the time under all noise and fading conditions, as reflected in the average of M-QAM modulation types in Tables 8 through 13.

The 256-QAM signal type, under all noise and fading conditions can be correctly identified 78.2% of the time for randomly chosen high or low SNR levels and 100 trials as reflected as the average of the 256-QAM types in Tables 8 through 13. When tests were run without fading conditions on specifically higher SNR levels (SNR range: 50dB to 100dB), the ability to successfully classify 256-QAM was increased to 99%. Under the same conditions, 16- or 64-QAM signal types were correctly identified as being M-QAM 99% of the time as seen in Table 8. When tests were run on conditions of no fading and specifically lower SNR levels (i.e., randomly chosen between 0dB and 8dB), the ability to successfully classify 256-QAM was reduced to 53%, as shown in Table 9. Similarly, 16- or 64-QAM signal types were correctly identified as being M-QAM types 63% of the time for high noise (SNR range:0dB to 8dB) and no fading (Table 9). Under Rayleigh fading conditions, and low noise (SNR range: 50dB to 100dB), the success rate for M-QAM signals is over 99%. The 256-QAM signals under the same conditions are successfully classified 99% of the time as well, both shown in Table 10. For Rayleigh fading conditions and high noise (SNR range: 0dB to 8dB), the success rate is reduced to 54% for M-QAM, and 60% for 256-QAM signals, as shown in Table 11. For Ricean

fading conditions, and low noise (SNR range: 50dB to 100dB), the success rate is 98% for M-QAM signals and 98% for 256-QAM signals, as reflected in Table 12. However, for Ricean fading conditions and high noise (SNR range: 0dB to 8dB), the success rate is reduced to 54% for M-QAM signals and 60% for 256-QAM signals, as shown in Table 13. These values are recorded in Tables 8 through 13 in Appendix C.

VII. CONCLUSIONS

This thesis discussed the components used in classifying digital modulation types in multipath fading environments as well as additive white Gaussian noise. The MATLAB and Simulink models generated the signals, modeled propagation through noisy channels, and sent these signals through a classification scheme that attempted to identify and classify these modulation types correctly. Results demonstrate the robustness of the higher order statistical features to various levels of noise and fading.

This work is yet another small milestone in a large body of research conducted in this area. The advances of computing power, advances in user-friendly mathematical modeling software and the continued research will continue to yield results as above. Future work or extensions of this model will need to provide a greater number of modern modulation types including orthogonal frequency division multiplexing, cyclical shift keying, trellis coded modulation and others. Also, the work could be extended to include real-world signals. Additionally, it might be beneficial to study the utility of neural networks to further classify QAM and FSK type signals. Finally, further research could be done to evaluate the world of frequency hopped signals. It would be ideal to mesh this program together with another program that finds an unknown signal in a frequency hopped modulation scheme (e.g., [25] - [26]).

THIS PAGE INTENTIONALLY LEFT BLANK

APPENDIX A: ROBUSTNESS OF CLASSIFICATION FEATURES TO DISTURBANCE AND NOISE

This appendix discusses the robustness of moments and cumulants to various levels of additive white Gaussian noise and two types of fading; Ricean fading and Rayleigh fading. As can be seen from the figures below, there is a very clear similarity between all the figures. It may also be observed that when there is very little noise, (i.e., high signal-to-noise ratio), the significantly different colored feature results are closer to the edges of the graph. However, when noise is much greater, the "hotter" red areas and "cooler" blue areas tend toward the center of the graph. This shows how, moments and cumulants are relatively resilient to noisy conditions. These graphics show only the results of a specific low SNR level of 0dB and a specifically higher SNR level of 100dB but they are fairly representative of what results obtained for lower or higher SNR levels.

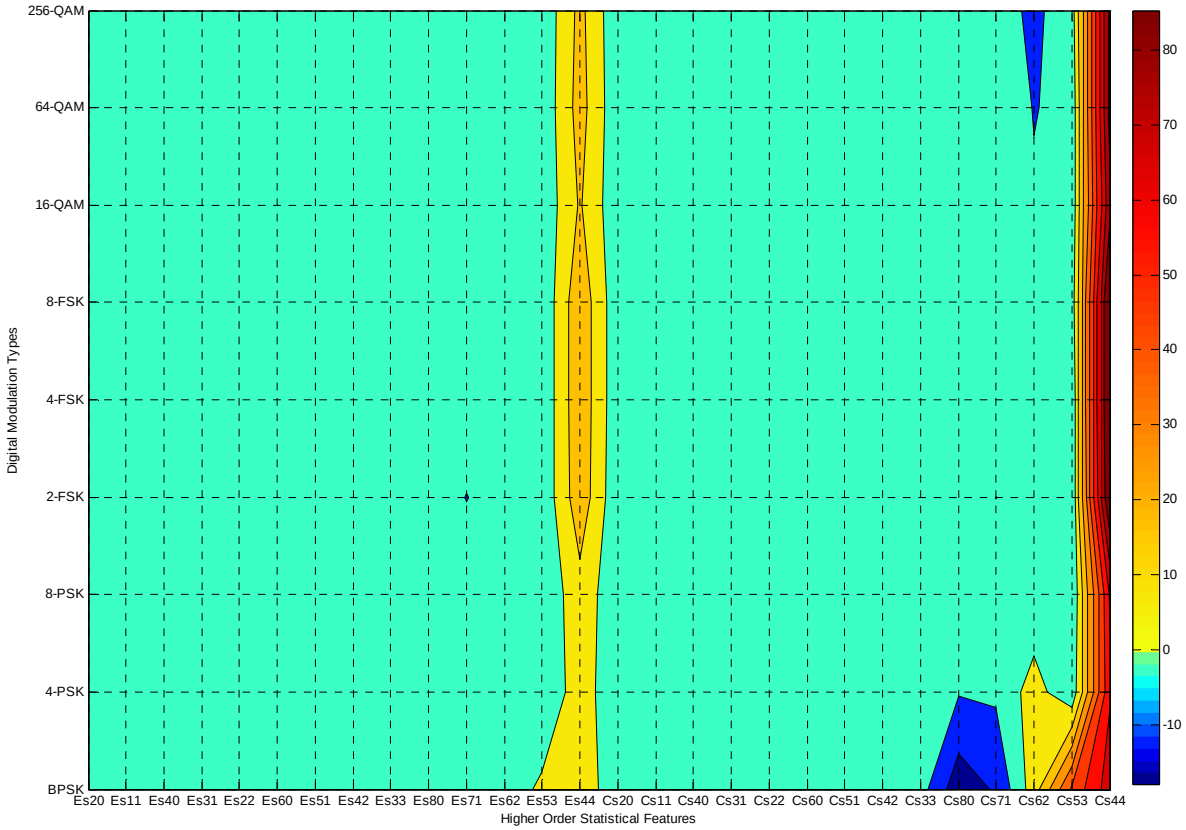

Figure 14. Surface Plot of Higher Order Statistics Against All Modulation Types Under No Fading and High Noise(SNR = 0dB)

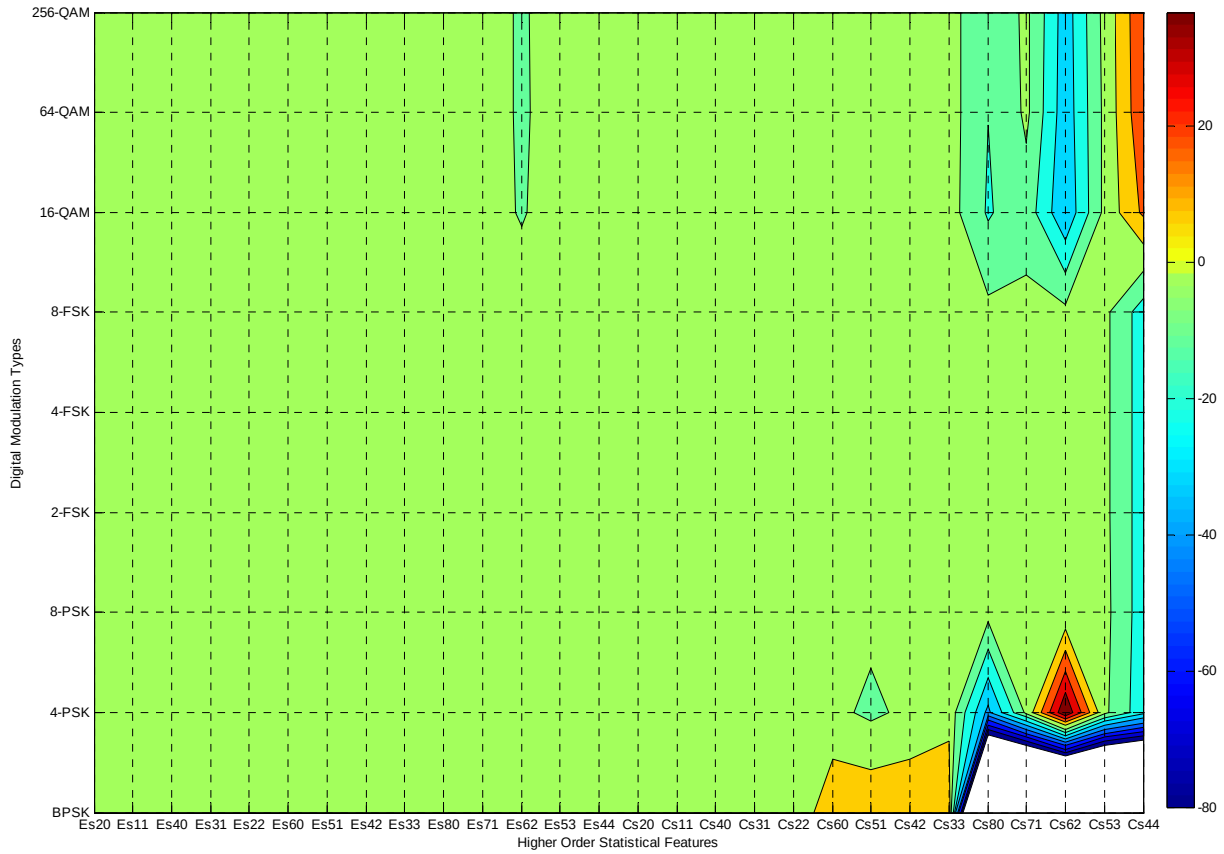

Figure 15. Surface Plot of Higher Order Statistics Against All Modulation Types No Fading and Low Noise(SNR = 100dB)

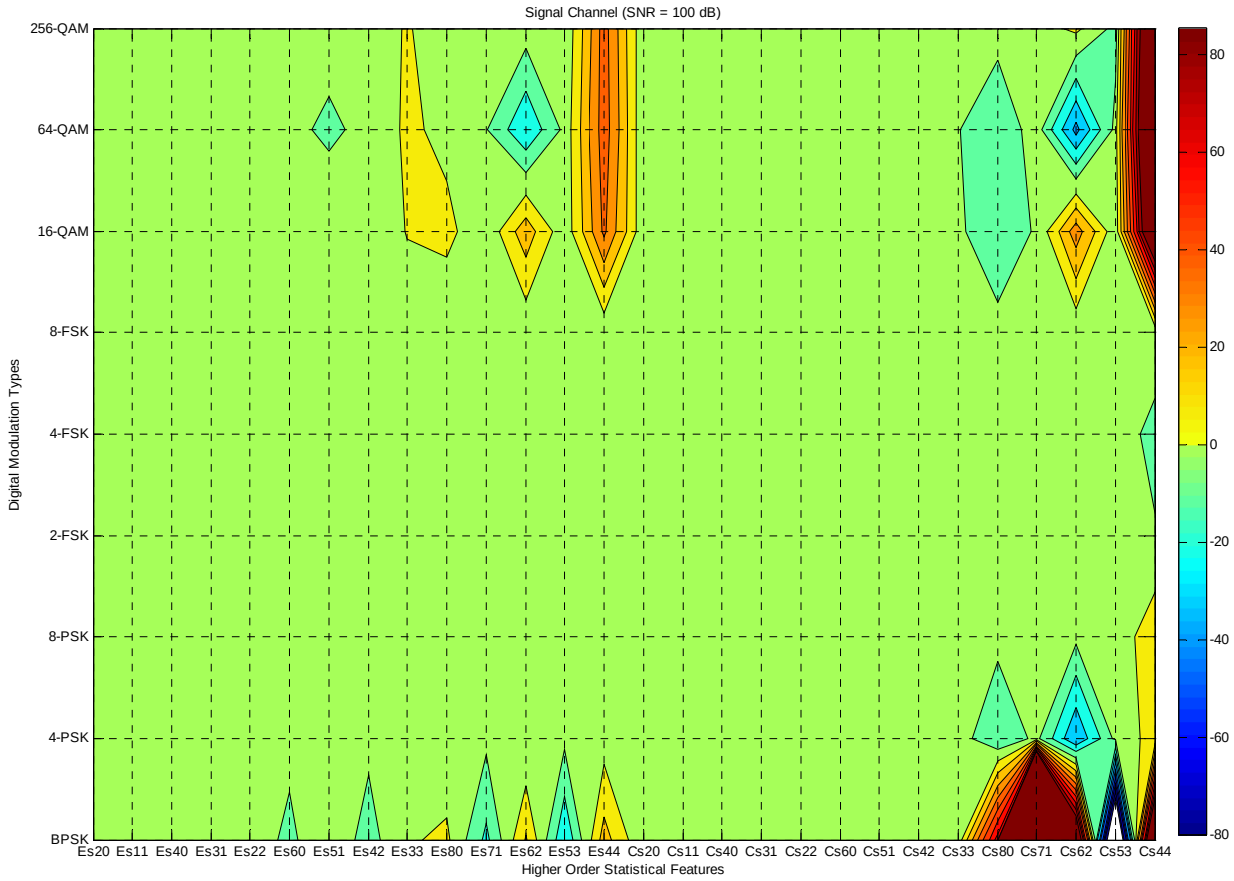

Figure 16. Surface Plot of Higher Order Statistics Against All Modulation Types Under Rayleigh Fading and Low Noise (SNR = 100dB)

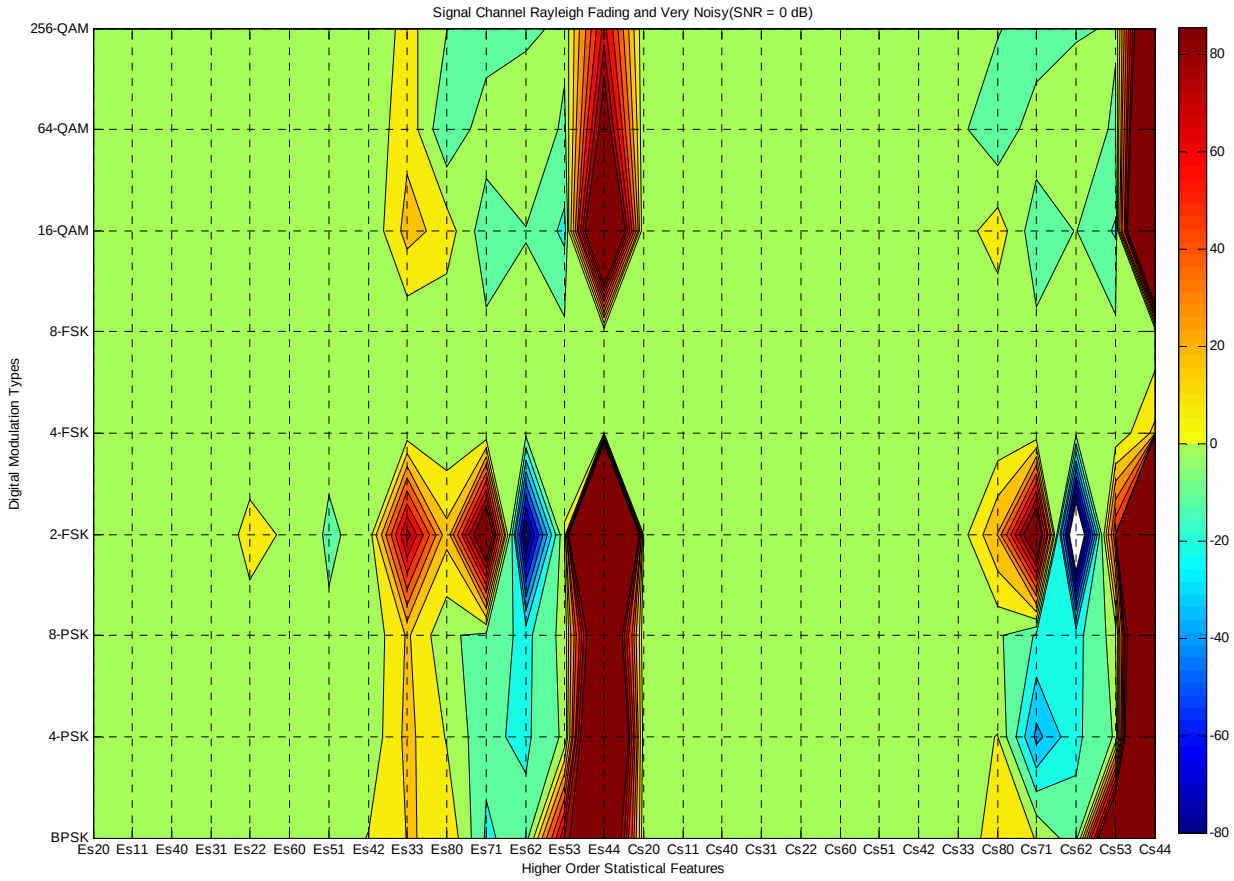

Figure 17. Surface Plot of Higher Order Statistics Against All Modulation Types Under Rayleigh Fading and High Noise (SNR = 0 dB)

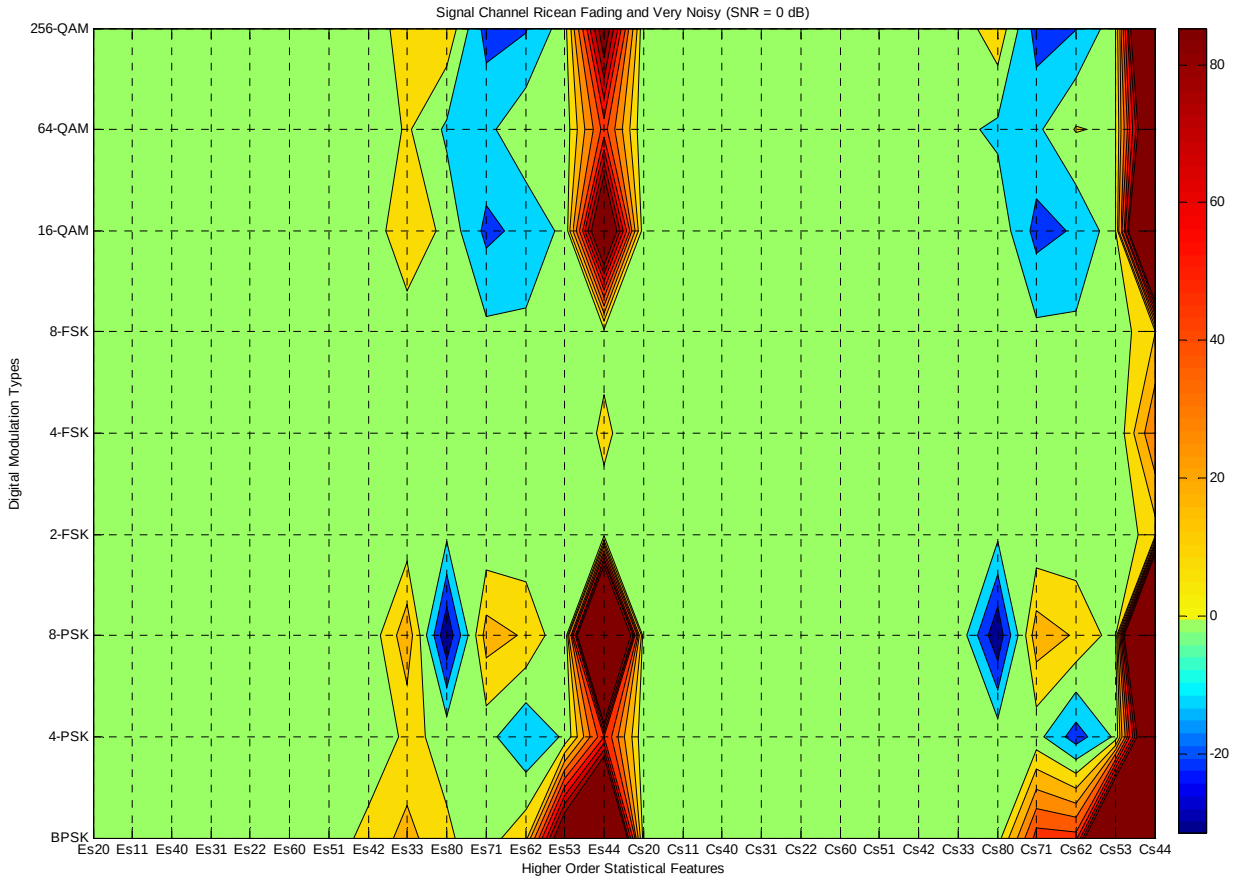

Figure 18. Surface Plot of Higher Order Statistics Against All Modulation Types Under Ricean Fading and High Noise (SNR = 0dB)

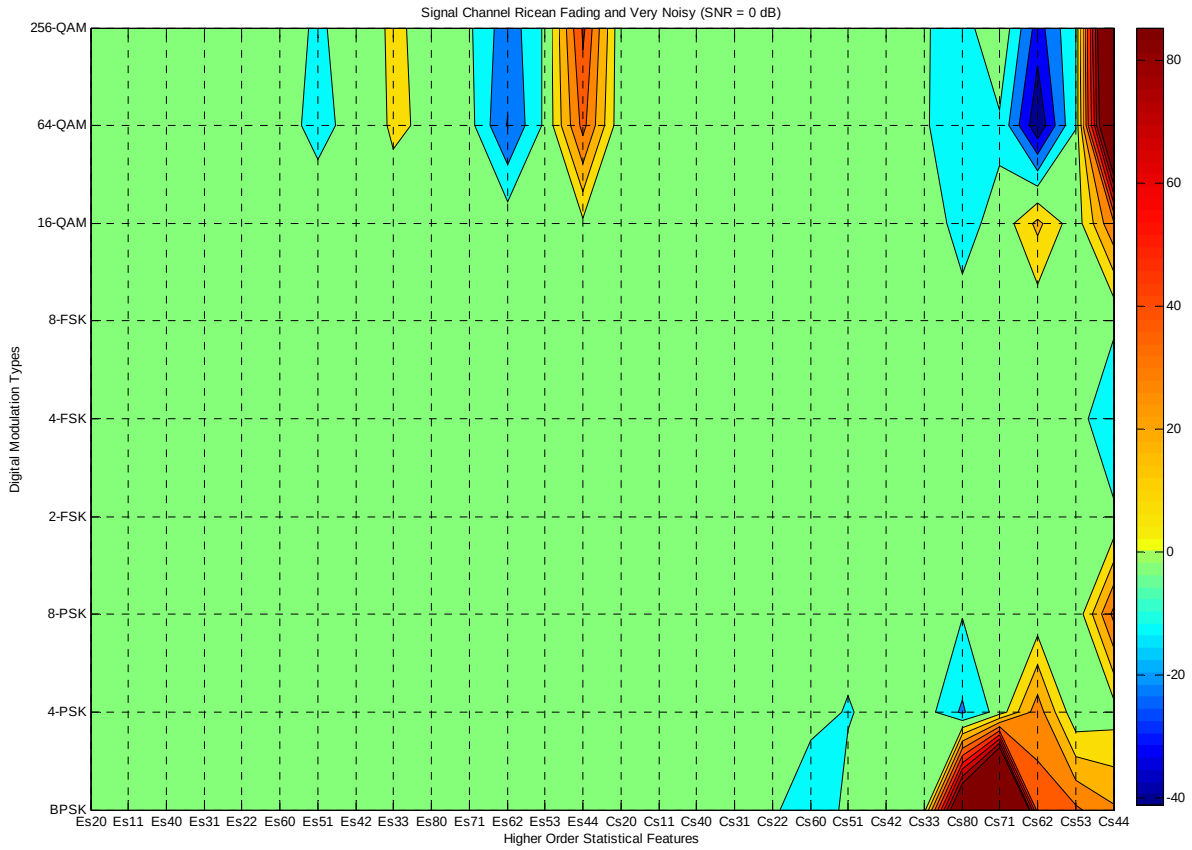

Figure 19. Surface Plot of Higher Order Statistics Against All Modulation Types Under Ricean Fading and Low Noise (SNR = 100 dB)

THIS PAGE INTENTIONALLY LEFT BLANK

`APPENDIX B: CLASSIFICATION THRESHOLDS

This appendix describes the process followed to determine the classification tree threshold values from the Figures included in Appendix A. The first step in gathering the classification thresholds used to identify the signal of interest was to plot the selected statistical feature values obtained for all modulation types (M-PSK, M-FSK, and M-QAM) considered. We selected a threshold value for the eighth order cumulant, $C_{s,8,0}$, to be less than -200 for the BPSK modulation type and re-plotted the figure with the BPSK type information eliminated to select the next threshold, leading to Figure 20 below.

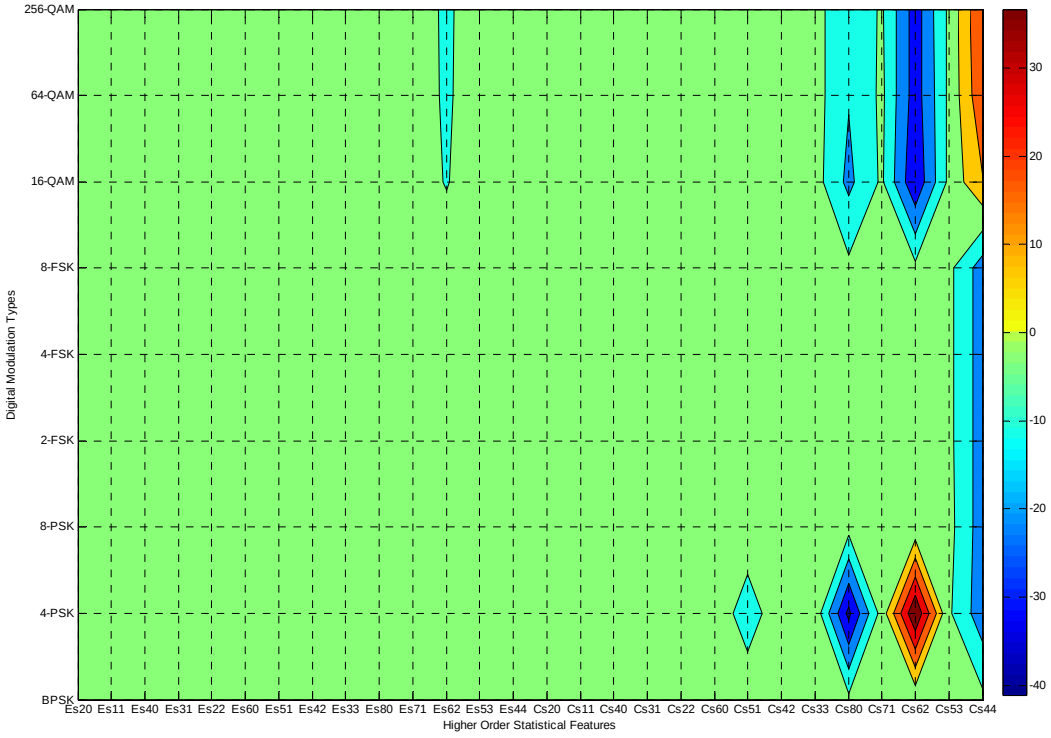

Figure 20. Surface Plot of Higher Order Statistics with BPSK Eliminated, Low Noise (SNR = 0dB), and No Fading

Figure 20 plots higher order statistics values against the digital modulation techniques, where the BPSK signal type has been removed. Note that features associated with the 4-PSK modulation type stand out against features associated with all other modulation types. 4-PSK modulated signals have an eighth order cumulant (i.e., $C_{s,6,2}$) which is significantly different from every other statistical features present. The 4-PSK signal has a large positive value (greater than thirty). Thus, thirty is chosen as the threshold to decide that an unknown signal is indeed 4-PSK. As noted in the results, this threshold value results in correct classification of the 4-PSK type 89% of the time, regardless of the noise level or fading level,. The remaining modulation types are eliminated, one by one in a similar fashion allowing the user to choose statistical thresholds.

APPENDIX C: CLASSIFICATION RESULTS

This appendix shows classification results obtained for the modulation types considered. The confusion matrix shows the actual signal types sent and associated decisions. Confusion matrices for the six different configurations considered are included in Tables 8 to 13 below. Table 8 corresponds to low noise and no fading conditions (SNR range: 50dB to 100dB). Table 9 corresponds to high noise (SNR range: 0dB to 8dB), and no fading. Table 10 corresponds to Rayleigh fading and low noise (SNR range: 50dB to 100dB) conditions. Table 11 corresponds to Rayleigh fading and high noise (SNR range: 0dB to 8dB) conditions. Table 12 corresponds to Ricean fading and low noise (SNR range: 50dB to 100dB) conditions. Finally, Table 13 lists results for Ricean fading and high noise (SNR range: 0dB to 8dB) conditions. Each trial was run 100 times and each table lists the number of decisions recorded. The percentage value for the overall classification rate listed in Tables 8 through 13 was computed by taking the arithmetic mean of the main diagonal of each table.

Classification Decision Overall Classification Rate: 99%	**True Signal Modulation Type Sent**					
	BPSK	4PSK	8PSK	MFSK	M QAM	256QAM
BPSK	100	0	0	0	0	0
4-PSK	0	100	1	0	0	0
8-PSK	0	0	98	0	0	0
M-FSK	0	0	1	98	1	1
16-QAM or 64-QAM	0	0	0	1	99	0
256-QAM	0	0	0	1	0	99

Table 8. Classification Results: Low Noise, No Fading, (100 Trials, SNR range: 50dB to 100dB)

Classification Decision Overall Classification Rate: 72.3%	**True Signal Modulation Type Sent**					
	BPSK	4PSK	8PSK	MFSK	M QAM	256QAM
BPSK	83	4	5	0	8	8
4-PSK	4	79	5	1	7	9
8-PSK	4	4	75	5	7	9
M-FSK	3	5	7	81	9	10
16-QAM or 64-QAM	4	5	3	8	63	11
256-QAM	2	3	5	5	6	53

Table 9. Success Results: High Noise, No Fading, (100 Trials, SNR range: 0dB to 8dB)

Classification Decision Overall Classification Rate: 99.2%	**True Signal Modulation Type Sent**					
	BPSK	4PSK	8PSK	MFSK	M QAM	256QAM
BPSK	100	0	0	0	0	0
4-PSK	0	99	0	0	0	0
8-PSK	0	1	100	1	0	0
M-FSK	0	0	0	98	0	0
16-QAM or 64-QAM	0	0	0	1	99	1
256-QAM	0	0	0	0	1	99

Table 10. Success Results: Low Noise, Rayleigh Fading, (100 Trials, SNR range: 50dB to 100dB)

Classification Decision Overall Classification Rate: 68.5%	**True Signal Modulation Type Sent**					
	BPSK	4PSK	8PSK	MFSK	M QAM	256QAM
BPSK	81	5	7	6	8	6
4-PSK	6	81	7	9	9	6
8-PSK	5	6	70	9	9	6
M-FSK	2	3	8	65	11	8
16-QAM or 64-QAM	3	3	1	6	54	11
256-QAM	3	2	0	5	9	60

Table 11. Success Results: High Noise, Rayleigh Fading, (100 Trials, SNR range: 0dB to 8dB)

Classification Decision Overall Classification Rate: 97.3%	**True Signal Modulation Type Sent**					
	BPSK	4PSK	8PSK	MFSK	M QAM	256QAM
BPSK	97	2	1	0	0	0
4-PSK	2	95	1	0	0	0
8-PSK	1	3	98	1	0	0
M-FSK	0	0	0	98	1	1
16-QAM or 64-QAM	0	0	0	1	98	1
256-QAM	0	0	0	0	1	98

Table 12. Success Results: Low Noise, Ricean Fading, (100 Trials, SNR range: 50dB to 100dB)

Classification Decision Overall Classification Rate: 67.5%	**True Signal Modulation Type Sent**					
	BPSK	4PSK	8PSK	MFSK	M QAM	256QAM
BPSK	75	1	7	7	4	1
4-PSK	9	79	9	7	8	8
8-PSK	6	8	70	6	8	10
M-FSK	5	7	8	67	10	10
16-QAM or 64-QAM	5	5	4	9	54	11
256-QAM	0	0	2	4	16	60

Table 13. Success Results: High Noise, Ricean Fading, (100 Trials, SNR range: 0dB to 8dB)

APPENDIX D: SOFTWARE IMPLEMENTATION DESCRIPTION

This appendix provides information on the MATLAB and Simulink codes used in this work. Following the model shown in Figure 13, we first generate the digital signals utilizing a Simulink model as illustrated in Figure 21. Noise distortions were also added at that point.

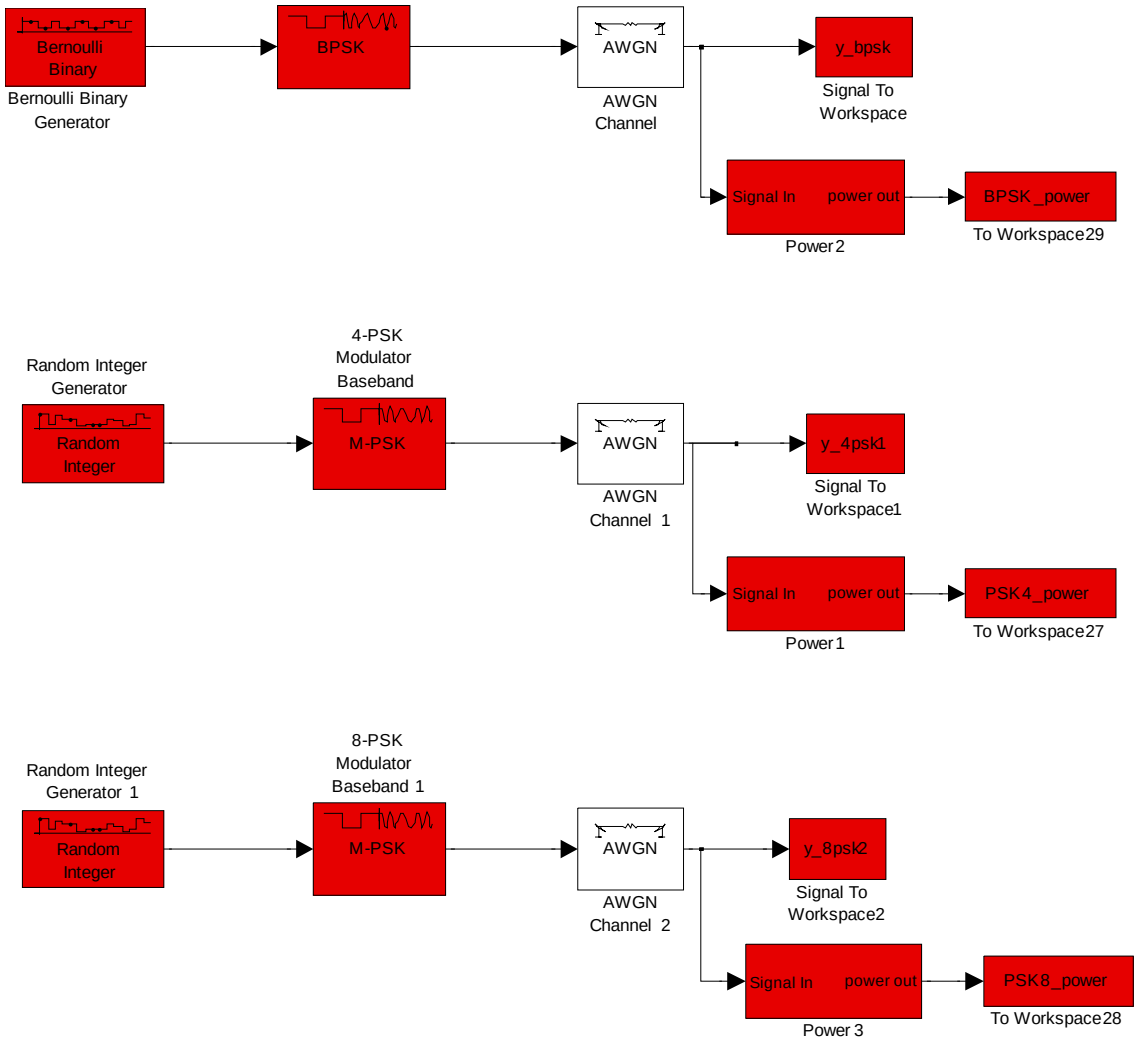

Figure 21. Simulink Model of Digital Signal Generator for PSK Signals (AWGN distortion only)

Multipath environments were simulated via the communications channel block representing the Rayleigh or the Ricean channel. This block was placed after the AWGN block. The next step was to choose a signal to evaluate which was done via an M-file. The next step in the programming process was to calculate the signal's higher order statistics which was also done via a Simulink model. This Simulink model consisted of three parts. The first part was the external shell, which receives the signal as an input. Although there appears to be no output, the outputs are actually generated inside a sub-system, or sub-blocks within the shell shown in Figure 24.

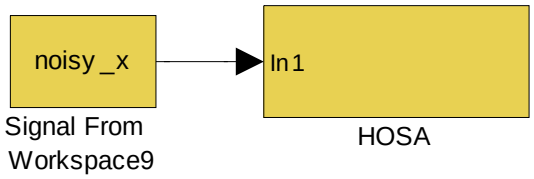

Figure 22. Outer Shell for Moments & Cumulants Which Receives Signal As Input

The internals to this outer shell, where HOSA stands for Higher Order Statistical Analysis is given in Figure 25. Again, the inputs are the signal of interest, and the outputs are workspace variables associated with the moments and cumulants evaluated in this research. The complete code and Simulink models can be obtained by contacting Professor Monique Fargues at NPS.

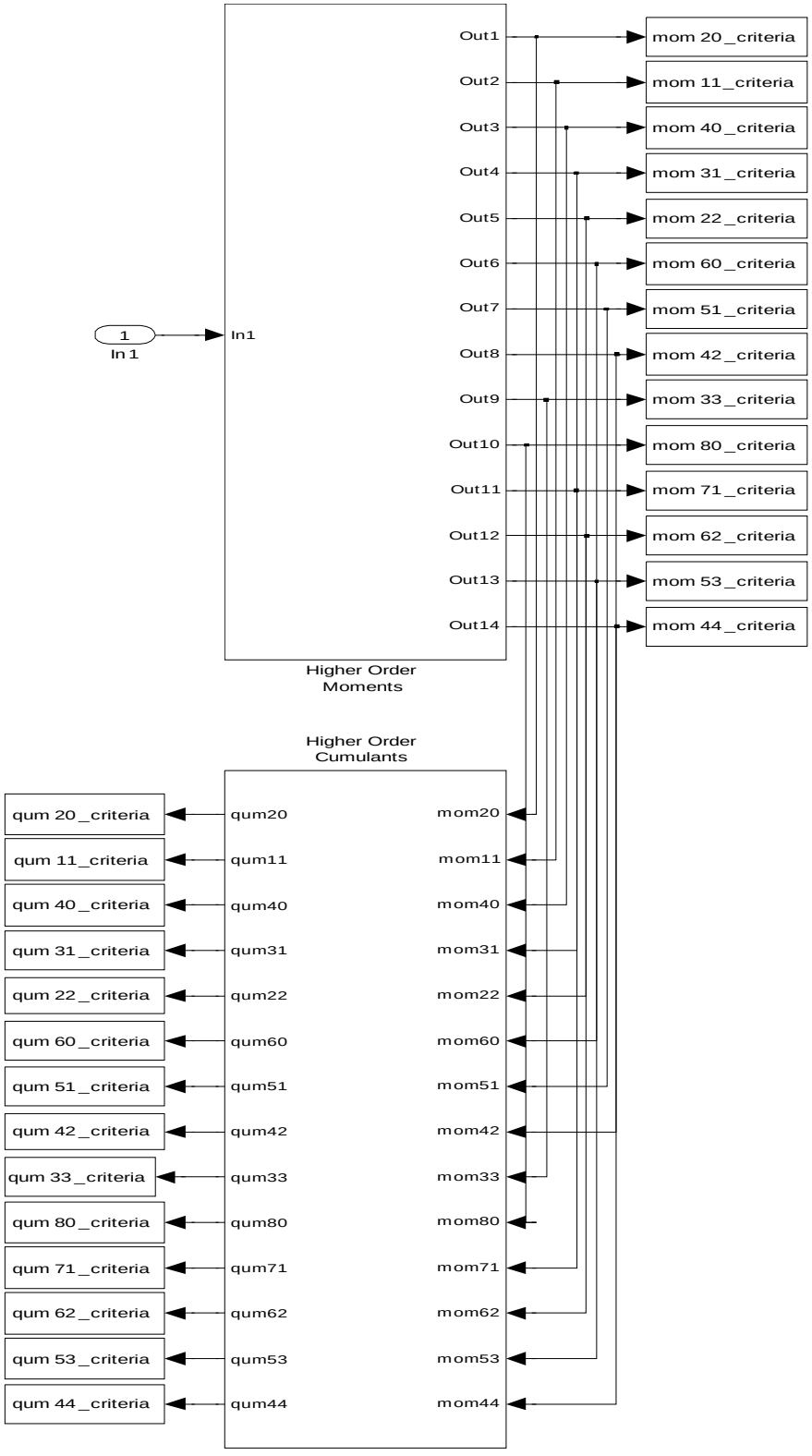

Figure 23. First Sub-Blocks which Receive Signals and Output HOS

Simulink blocks designed to compute the fourth order cumulants ($C_{s,a,b}$) and moment ($E_{s,a,b}$) are shown in Figures 8 and 9. Next, moments and cumulants were normalized with respect to the signal power. These normalized moments and cumulants were then processed by the classification program, with corresponding threshold values as described in Appendix A and B.

LIST OF REFERENCES

[1] G. Hatzichristos, *Classification of Digital Modulation Types in Multipath Environments,* Electrical Engineering MSEE Thesis, Naval Postgraduate School, Monterey, CA, 2001.

[2] F. Liedtke, "Computer simulation of an automatic classification procedure for digitally modulated communication signals with known parameters", *Signal Processing,* vol. 6, pp.311-323, 1984.

[3] C. Le Martret, D. Boiteaut, "Modulation classification by means of different orders statistical moments," *IEEE Military Communications 1997,* Monterey, Nov. 2-4, pp. 256-258, 1997.

[4] P. Marchand, *Détection et Reconnaissance de Modulations Numériques a l'aide des Statistiques Cycliques d'ordre Supérieur*, Thése de l'Institut National Polytechnique de Grenoble, 1998.

[5] S. Taira, E. Murakami, "Automatic classification of analogue modulation signals by statistical parameters," Second Research Center, Technical Research and Development Institute, Japan Defense Agency, Tokyo, Japan, 1999.

[6] W. Wei, J. Mendel "Maximum-likelihood classification for digital amplitude-phase modulations," *IEEE Transactions on Communications*, vol. 48, no. 2, pp. 127-129, 2000.

[7] V. Kalinin, D. Kavalov, "A SAW neural network processor for classification of MSK and BPSK modulations," *Proceedings of 2002 IEEE International Ultrasonics Symposium*, vol. 1, pp. 263 – 266, 2002.

[8] O. Dobre, Y Bar-Ness, S. Wei, "Robust QAM modulation classification algorithm using cyclic cumulants," *IEEE Wireless Communications and Networking Conference*, vol. 2, pp. 745 – 748, 2004.

[9] S. Baarrij, F. Nasir, S. Masood, "A robust hierarchical digital modulation classification technique: using linear approximations," *IEEE International Symposium on Signal Processing and Information Technology*, pp. 545 – 550, 2006.

[10] B. Sklar, *Digital Communications: Fundamentals and Applications,* Pearson Education, India, 2001.

[11] W. Stallings, *Data and Computer Communications*, Pearson Education, New Jersey, 2007.

[12] Wikipedia – The Free Encyclopedia, "Bell 103 Modem," April 2008, [Online] http://en.wikipedia.org/wiki/Bell_103_modem.

[13] F. Xiong, *Digital Modulation Techniques*, Artech House, Inc, Norwood, Massachusetts, 2006.

[14] Wikipedia – The Free Encyclopedia, "Pulse Shaping," December 2007, http://en.wikipedia.org/wiki/Pulse_shaping.

[15] S. Haykin, M. Moher, *Introduction to Analog & Digital Communications*, John Wiley & Sons, Inc., 2007.

[16] MATLAB Help Documents, *Communications Toolbox*, 2007.

[17] Wikipedia – The Free Encyclopedia, "Rayleigh Fading," May 2008, http://en.wikipedia.org/wiki/Rayleigh_fading.

[18] C. Kao, "Performance of the *IEEE 802.11a* wireless LAN standard over frequency-selective, slow Ricean-fading channels," Electrical Engineering MSEE Thesis, Naval Postgraduate School, Monterey, CA, 2002.

[19] J. Proakis, *Digital Communications 4th Edition*, McGraw-Hill, New York, 2001.

[20] P. Meyer, *Introductory Probability and Statistical Applications*, Addison-Wesley Publishing Co., Reading, MA, 1970.

[21] A. Hald, *The Early History of the Cumulants and the Gram-Charlier Series*, International Statistical Review, vol. 68, pp. 137-153, 2000.

[22] Wikipedia – The Free Encyclopedia, "Cumulant," June 2008, http://en.wikipedia.org/wiki/cumulant.

[23] Weisstein, Eric W. "Fourier Transform." From *MathWorld*--A Wolfram Web Resource. http://mathworld.wolfram.com/FourierTransform.html, 2005.

[24] P. Valz, A.I. McLeod, and M. Thompson, "Cumulant generating function and tail probability approximations for Kendall's score with tied rankings," *The Annals of Statistics*, vol 23, Number 1, pp. 144-160, 1995.

[25] C. Brown, *Detection Of Frequency-Hopped Signals Embedded In Interference Waveforms*, Electrical Engineering MSEE Thesis, Naval Postgraduate School, Monterey, CA, 2005.

[26] K. Waters, *Narrow Band Filtering Effects On Frequency Hopped Signals*, Electrical Engineering MSEE Thesis, Naval Postgraduate School, Monterey, CA, 2002.

[27] Wikipedia – The Free Encyclopedia, “Biological Neuron,” May 2008, http://en.wikipedia.org/wiki/Neuron

[28] S. Kartalopoulos, *Understanding Neural Networks and Fuzzy Logic*, IEEE Press, Piscataway, NJ, 1996.

THIS PAGE INTENTIONALLY LEFT BLANK

INITIAL DISTRIBUTION LIST

1. Defense Technical Information Center
   Ft. Belvoir, Virginia

2. Dudley Knox Library
   Naval Postgraduate School
   Monterey, California